Salado *et al. Energy Mater* 2023;3:300037
DOI: 10.20517/energymater.2023.36

Energy Materials

Review

Open Access

Check for updates

Advanced and sustainable functional materials for potassium-ion batteries

Manuel Salado[1,2,#,*], Marco Amores[2,#], Cristina Pozo-Gonzalo[2], Maria Forsyth[2,3], Senentxu Lanceros-Méndez[1,3]

[1]BCMaterials, Basque Center for Materials, Applications and Nanostructures, UPV/EHU Science Park, Leioa 48940, Spain.
[2]Institute for Frontier Materials, Deakin University, Burwood 3125, Australia.
[3]IKERBASQUE, Basque Foundation for Science, Bilbao 48013, Spain.
[#]Authors contributed equally.

***Correspondence to:** Dr. Manuel Salado, BCMaterials, Basque Center for Materials, Applications and Nanostructures, UPV/EHU Science Park, Leioa 48940, Spain. E-mail: manuel.salado@bcmaterials.net/manuel.saladomanzorro@deakin.edu.au

How to cite this article: Salado M, Amores M, Pozo-Gonzalo C, Forsyth M, Lanceros-Méndez S. Advanced and sustainable functional materials for potassium-ion batteries. *Energy Mater* 2023;3:300037. https://dx.doi.org/10.20517/energymater.2023.36

Received: 5 May 2023 **First Decision:** 29 May 2023 **Revised:** 17 Jun 2023 **Accepted:** 4 Jul 2023 **Published:** 1 Sep 2023

Academic Editors: Sen Xin, Federico Bella, Hong Xu **Copy Editor:** Fangling Lan **Production Editor:** Fangling Lan

Abstract

Rechargeable potassium-ion batteries (PIBs) have gained attention as sustainable, environmentally friendly, and cost-effective large-scale stationary energy storage technology. However, although this technology was assumed to perform in a manner similar to that of its monovalent counterparts, huge anode volume expansion and sluggish kinetics are posing challenges in up-scaling it. Apart from the efforts to develop and optimise electrode materials, recent research endeavours have also focussed on the essential role of sustainability. These attempts have often relied on bio-derived and bio-inspired materials to mimic the effectiveness of nature. Furthermore, the use of materials with self-healing properties can alleviate electrode degradation after cycling and augment its electrochemical performance. This review summarises the development of smart materials with self-healing properties that aid in overcoming the present issues of PIBs and highlights the relevance of the interphases. In addition, state-of-the-art design strategies for bio-derived and bio-inspired materials are presented and discussed. The incorporation of recycled and sustainable materials into the manufacturing of PIBs is expected to contribute towards the ultimate goal of achieving truly circular economy ecosystems. Finally, perspectives for further advancements are provided to kindle new ideas and open questions regarding the use of new-generation materials in the development of PIBs.

Keywords: Potassium batteries, self-healing, polymers, sustainable, bio-inspired, circular economy

INTRODUCTION

Energy-storage solutions are the need of the hour for meeting the continuously increasing worldwide energy demand, supporting the transition towards electrification of transportation and addressing the issue of global warming. Lithium-ion batteries (LIBs) currently represent the preferred energy storage technology owing to their high energy density, low long-term self-discharge, wide operable temperature range, technology maturity, *etc.*[1]. The rapid increase in the demand for batteries for electric transport is predicted to strain the supply chain of already scarce materials for LIBs[2]. This fact, together with environmental and sustainability concerns, is driving research endeavours towards alternative alkali-metal batteries with more abundant active material components[3,4]. Lower-cost alkali-metal technologies relying on heavier cations can complement lithium-ion technologies in spaces where the price is the major driving factor with lower requirements for weight and space, such as in stationary energy storage applications. This is the case of sodium-ion batteries (NIBs); despite their lower theoretical and practical energy density compared to LIBs [Figure 1A][5], NIBs are close to commercialisation owing to their projected lower price based on the high abundance of Na-, cobalt (Co)-, and Ni-free cathode materials[4].

Potassium-ion batteries (PIBs), with a more negative redox potential [-2.93 V *vs.* standard hydrogen electrode (SHE)] than that of Na and comparable to that of Li [Table 1], are also a promising energy-storage technology that will positively influence the battery potential. More importantly, potassium (K) is the seventh most abundant element on the earth's crust, which has a wide global distribution and provides energy equity resources. Furthermore, the major chemical components present in PIBs are widely available [Figure 1B]. PIBs have the added advantage of not requiring copper-based current collectors on the anode and using cheaper and lighter Al because potassium does not alloy with it. Also, the higher mass-to-charge ratio, together with a smaller solvated radius[6], permits the higher conductivity of K^+ in carbonate liquid electrolytes (> 15.2 mS·cm^{-1}) with low desolvation energy [Table 1][8]. The first functional PIB prototype was developed in 2004 by Eftekhari using an organic electrolyte and a Prussian blue (PB)-based cathode material with potassium metal anodes[13]. However, research attention was shifted to NIBs until 2015, when the interest in PIBs reawakened, fuelled by reports on the intercalation of K^+ on graphite as anode materials in organic electrolytes[14,15]. These promising features and the potential of PIB technology have led to commercial attempts, with start-up Group 1 announcing their plans to launch their first prototype by 2027[16]. The basic electrochemical operation of a PIB based on a graphite electrode paired with a PB analogue (PBA) cathode is based on the electrochemical (de)intercalation of K^+ within the host electrode materials following the classical rocking chair intercalation mechanism, as summarised in Eq. 1 for the charge and discharge processes[17].

Charge mechanism

Graphite anode: $8C + K^+ + e^- \rightarrow KC_8$

PBA cathode: $K_2Mn^{2+}[Fe_2{+}(CN)_6] \rightarrow Mn^{3+}[Fe^{3+}(CN)_6] + 2K^+ + 2e^-$

Discharge mechanism

Graphite anode: $KC_8 \rightarrow 8C + K^+ + e^-$

PBA cathode: $Mn^{3+}[Fe^{3+}(CN)_6] + 2K^+ + 2e^- \rightarrow K_2Mn^{2+}[Fe^{2+}(CN)_6]$

Equation 1 Charge and discharge reaction mechanisms for a graphite||PBA-based PIB.

Table 1. A comparative summary of the properties of Li, Na, and K alkali-metal elements and their cations

	Li	Na	K
Earth's crust availability (%$_{wt}$)	0.0017	2.4	2.09
Geographical distribution	South America, Australia, China	Widely available	Widely available
Relative atomic mass	6.94	23.00	39.10
Shannon's ionic radii (Å)	0.76	1.02	1.38
Stokes radii in PC (Å)[6]	4.8	4.6	3.6
E^0 ($A^+_{aq.}$/A) (V) *vs.* SHE	-3.04	-2.71	-2.93
E^0 (A^+_{PC}/A) (V) *vs.* Li^+_{PC}/Li[7]	0	0.23	-0.09
Melting temperature (°C)	180.5	97.7	63.4
Desolvation energy PC electrolyte (kJ·mol^{-1})	215.8	158.2	119.2
Conductivity in PC (mS·cm^{-1})[8]	8.3	9.1	15.2
Coordination preference of A^+ in $AMeO_2$	Octahedral Tetrahedral	Octahedral Prismatic	Prismatic
Cost of carbonate salt (US$·ton^{-1})[9]	6,500	200	1,000
Cost of industrial grade metal [US$·ton^{-1})[10]	245,533	16,150	165,000
Graphite theoretical capacity (Ah·kg^{-1})[11]	372	112	279
MC_6-$MCoO_2$ theoretical capacity (Wh·kg^{-1})[12]	279	231	218

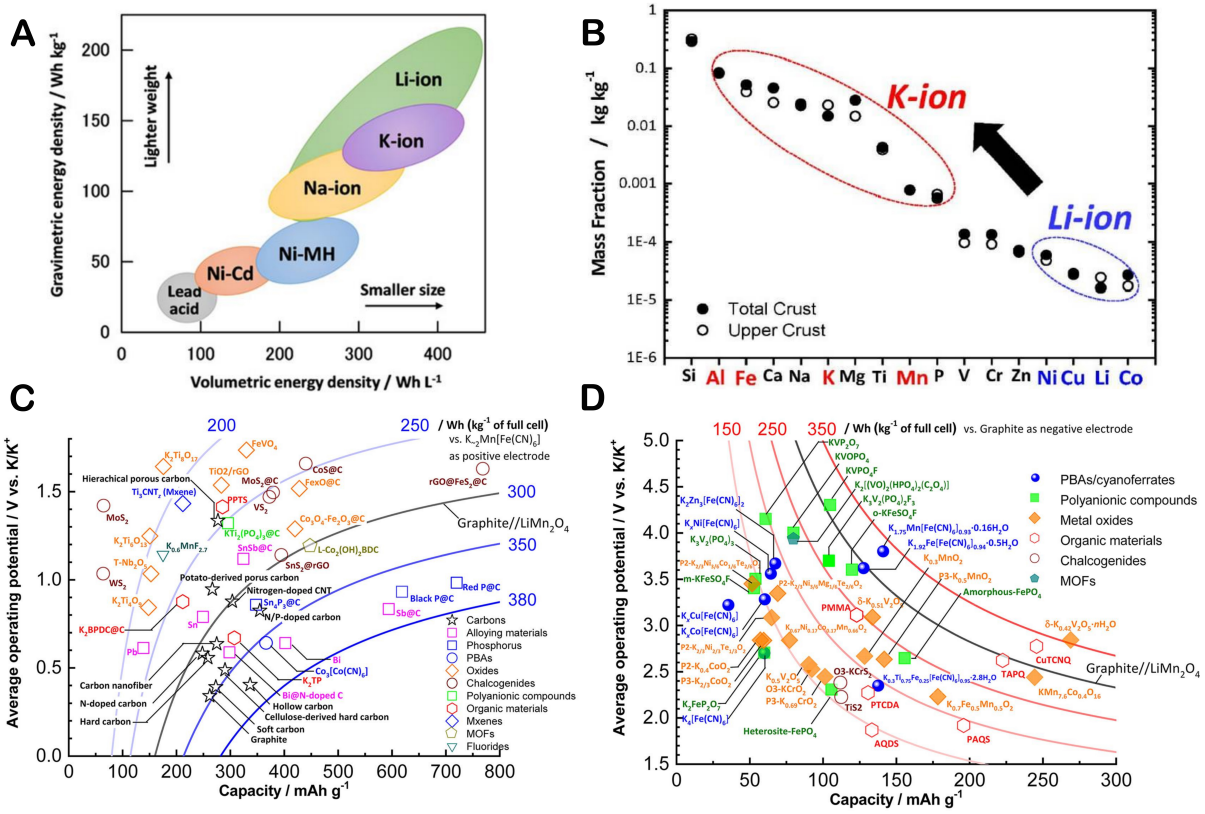

Figure 1. (A) Energy density plot of different rechargeable battery technologies (reprinted with permission[5]). (B) Abundance of the most common elements in PIBs and LIBs within the earth's crust (reprinted with permission[5]). (C and D) Anode and cathode electrodes and their achieved energy densities, capacities, and working potentials in PIBs (adapted with permission from[18]).

Figure 1C and D[18] provides a global view of the wide range of electrode materials that have been explored for use in PIBs, where energy densities close to 350 $Wh{\cdot}kg^{-1}$ can be achieved. Research on cathode materials for PIBs has been centred on three leading families of materials, namely, PBAs, layered oxides, and polyanionic host materials.

PBA materials $[K_xM[M'(CN)_6]_{1-y}{\cdot}z{\cdot}H_2O$ M, where M′ = Fe, Mn, or Ni, y is the number of $[M'(CN)_6]^{n-}$ vacancy, and z is the number of H_2O molecules, either occupying the K sites (interstitial water) or coordinating to the M metal at vacancy sites (coordinated water), present a cubic structure with large interstitial sites in which K can be (de)inserted by an intercalation mechanism. PBAs can reach redox operating voltage potentials close to 3.9 V *vs.* K^+/K and capacities of 140 $mAh{\cdot}g^{-1}$, which enables energy densities comparable to those of $LiCoO_2$. The presence of structural water and Mn dissolution, however, hinders the true potential of PBAs because of unwanted side reactions and reduces their cyclability[19]. Layer oxide materials are analogous to those employed in LIBs and have also been explored for use in PIBs. K_xMO_2 (M = Mn, Ni, Co, or Cr) layered-oxide crystal structure can be classified according to Delmas notation[20] as O3-, P2-, and P3-type depending on the coordination geometry of the intercalated alkali metal (octahedral or prismatic)[21]. In the case of K^+, its larger size can be better accommodated within the trigonal prismatic sites, which makes the P-type structures more desirable for use as cathode host materials with K^+ intercalation. Operating redox potentials are, however, usually < 3.5 V *vs.* K^+/K, which limits the energy density of the system[22]. Polyanionic materials [$KMXO_4$ with (M = transition metals) and $(XO_4)^{n-}$ (X = P, S, As, Si, Mo, or W)] can produce structures with high operating potentials of > 4 V *vs.* K^+/K and capacities of > 100 $mAh{\cdot}g^{-1}$ upon K^+ intercalation[23]. Careful selection of the polyanionic polyhedral moieties and the tailoring of anions can produce open frameworks for rapid K^+ diffusion at high voltages. Fluorination of these polyanionic materials to produce sulphate fluorides, $KMSO_4F$ (M = Fe, Co, or Ni), has also been explored, where up to 0.8 K^+ could be intercalated per formula unit[24]. Other recently investigated cathode materials include organic-based materials, such as small molecules, metal-organic frameworks (MOFs), and polymers. These organic-based materials are versatile and are an environmentally friendly alternative to conventional metal-based electrodes. This type of electrode, however, faces the problems of low operating voltages, dissolution issues, and poor electronic conductivity[25].

Similar to the Li and Na systems, K-chalcogenide (K-S, K-Se) batteries have also been explored[26,27], promising cathode energy densities of > 1,000 $Wh{\cdot}kg^{-1}$ via chalcogen to K_xS or K_xSe conversion reactions[26]. The pitfalls in this type of chemistry are similar to those of Li and Na chemistries, with the shuttle effect of polysulfides limiting the cycling life performance.

Regarding anodes, carbon-based materials have been extensively studied and are the preferred choice because of their low redox potential *vs.* K^+/K. Unlike Na^+, K^+ can effectively and readily intercalate into graphite, with a potential of < 0.5 V *vs.* K^+/K and capacities of c.a. 279 $mAh{\cdot}g^{-1}$[8,9]. The larger solid-state radii of K^+, however, results in graphite volume expansions of up to 61% upon potassiation, which is six times larger than that of lithiation[8]. Hard carbons can offer larger capacities than graphite via additional K^+ adsorption onto the carbon surfaces. This adsorption is, however, obstructed in practical applications by higher overpotentials and lower initial Coulombic efficiencies[28]. The potassium metal anode offers the lowest redox potential possible for PIBs via the platting/stripping mechanism, with a capacity higher than that of graphite (687 $mAh{\cdot}g^{-1}$). Nonetheless, the potassium metal faces the same challenges as its Li and Na counterparts, with the dendritic formation of deposits and the added increased reactivity towards oxygen and water and the low melting temperature (63.5 °C). Conversion materials (metal oxides and allowing metals (Sn, Si, Ge, Bi, Sb, and P) can offer high theoretical specific capacities of up to 2,596 $mAh{\cdot}g^{-1}$ (K_3P system)[29]. Nevertheless, these materials undergo large volume changes of > 600% during cycling owing to

the formation of new chemical entities via the conversion reaction (e.g., $MX + K^+ + e^- \rightarrow M^0 + KX$). This reaction results in poor cyclability; therefore, strategies to alleviate the negative impact of the volume change are needed[30].

Electrolyte development is essential to attain the highest possible performance for each class of electrode materials. The majority of the reported studies are based on the use of liquid electrolytes composed of alkyl carbonates or ethers with common potassium salts that are analogous to those employed in LIBs and NIBs, such as KPF_6, KBF_4, or KFSI (potassium bis(fluorosulfonyl)imide)[13,31]. Advanced liquid electrolyte compositions, such as ionic liquids, have also been explored to improve the compatibility with potassium metal and high-voltage cathodes[32,33]. The adequate selection of the salt in the liquid electrolyte is critical for the performance of PIBs. The chemistry of the salt anion can influence the conductivity of K^+ in the electrolyte, the transport number and the composition of the solid-electrolyte interphase (SEI) formed at the electrode interface during battery operation. For instance, KFSI provides higher conductivity compared to KPF_6[34], KPF_6 offers good passivation of the Al current collector at high voltages, and KFSI has been shown to be corrosive[35]. KPF_6 is highly sensitive to oxygen and moisture and can easily decompose to HF, PF_5, and POF_3. On the contrary, KFSI has been reported to be a more stable SEI than KPF_6 in alloy-based anode materials[36]. These differences in properties show that the salt employed in the electrolyte needs to be selected by considering the whole chemistry of the battery.

The choice of solvent(s) is also critical in PIB performance. Of the carbonate solvents, ethylene carbonate/propylene carbonate (EC/PC) mixtures have been shown to facilitate higher cycling performance of the graphite anode compared with EC/dimethyl carbonate (DMC) or EC/DEC solvent mixtures owing to the formation of a more stable SEI[37]. Furthermore, the use of additives in the electrolyte can enhance the stability of the SEI formed at the interface of the PIB electrodes. Small amounts of ethylene sulphate, in conjunction with trimethyl phosphate in KFSI/trimethyl phosphate (TMP) electrolyte, have been reported to improve the cycling of graphite anode upon potassium intercalation because of the formation of a more robust SEI that decreases K^+-solvent co-intercalation[38].

Similar to the case of Li or Na chemistries, solid-state electrolytes have also been explored in K batteries to improve the safety and performance of potassium metal anode systems or alleviate the shuttle effect of polysulfides on K-S chemistries, for instance[39-42].

The environmental appeal of K batteries is not limited to the higher abundance of the element and the electrode components and extends to the entire life cycle of the technology and its long-term sustainability. Hence, the current cyclability of non-aqueous PIBs falls well behind that of mature LIB technology owing to its shorter long-term cycling performance. Some of the key reasons are the larger size of the K-ion, which produces higher strain and larger volume changes within the host electrodes during solid-state diffusion. Moreover, the high reactivity of the potassium metal anode results in a higher number of parasitic reactions, which lead to premature degradation and failure of the cell[43,44].

To overcome these challenges and improve the performance and sustainability of the PIB technology, it is pivotal to design novel advanced materials. These functional materials must be able to accommodate large volume changes and minimise parasitic reactions during the battery operation. Ideally, these materials should also possess self-healing properties to repair any damage resulting from battery cycling or any external damage. For instance, self-healing materials have been explored for other alkali-metal battery technologies in recent years, and their use allows the reversion of unavoidable degradation processes/ageing due to the operation of the battery cells in different environments[45].

In the last few decades, bio-inspired materials have gained immense attention within the energy storage community[46]. These materials can mimic specific morphologies, and nanoparticles with complex structures derived from nature have been proven to alleviate some of the degradation issues in LIBs and improve the kinetics in sluggish systems[47]. Sourcing battery materials from recycled materials or from biomass can further enhance the sustainability and competitiveness of PIBs. The research community is experimenting with the use of recycled materials in LIBs, and governmental and industrial initiatives are also being developed[48]. Apart from the use of recycled materials, biomass-derived materials have also been explored to produce low-cost electrode materials in other battery chemistries. Therefore, there are numerous opportunities for additional sustainable pathways to PIBs[49].

In this review, we aim to provide an up-to-date overview of the investigations on the applications of sustainable functional materials, including self-healing and bio-inspired materials in PIBs and sustainability routes to materials from biomass sources and recycled sources. The exploitation of such materials plays a crucial role in the design of next-generation energy storage devices, thus meeting the global demand for sustainable power solutions.

FROM NANOSTRUCTURED TO BIO-INSPIRED MATERIALS

To prevent capacity loss and disruption of the electrolyte/anode SEI, it is imperative to preserve the framework and interphase structures despite the substantial volume changes occurring in PIBs. Nanostructured conversion materials and hollow nanostructures have been extensively applied in different energy storage technologies owing to their advantage of increasing the surface contact area. Consequently, the transport of ions or electrons is favoured, and strains (volume expansion) associated with ion (Li^+, Na^+ or K^+) insertion are accommodated[50].

For instance, nanoheterostructures in which a nano-sized coordination polymer is combined with an inorganic material have recently attracted research attention for developing advanced materials for energy storage[51]. Specifically, size- and shape-controlled crystallisation of PB and its analogues can aid in overcoming the issues discussed in the previous section. Ming *et al.* successfully demonstrated that by tuning the pH of the electrolyte solution, the concentration of $K_3[Fe(CN)_6]$ and the presence of polyvinylpyrrolidone permits controlling the size of PB nanoparticles in the range of 20-200 nm, the surface area of 100 nm nanoparticles being 260 $m^2 \cdot g^{-1}$[52]. Mn-Ni PBA nanoparticles have been synthesised using the anion exchange method to improve K^+ diffusion kinetics and enhance the cycling performance [Figure 2A and B][53]. When the material was used as a cathode, it had an initial discharge capacity of 130.6 $mAh \cdot g^{-1}$ at 10 $mA \cdot g^{-1}$ and exhibited enhanced capacity retention (e.g., 83.8%) after 500 cycles.

Regarding the anode material used in PIBs, carbon materials (e.g., graphite, graphene, hard and soft carbon, and carbon nanotubes) have shown enormous potential[28]. Nevertheless, different strategies have been developed to improve their performance. Some promising results include the deposition of Bi_2S_3 nanorods on reduced graphene oxide[54], Bi@Bi_4Se_3@C nanoparticles[Figure 2C][55], flexible N-doped carbon/bubble-like MoS_2 core/sheath frameworks (MoS_2/NCS)[41], and the synthesis of complex hollow structures (e.g., dual-shell bismuth boxes [Figure 2D-F])[56]. Compared with simple hollow structures, complex ones (e.g., multi-shelled structures, yolk@shell/frame structures and superstructures) provide greater possibilities for customising their physicochemical properties via microscale/nanoscale structural manipulation. This possibility opens up new avenues for introducing novel functionalities or achieving enhanced performance in specific applications.

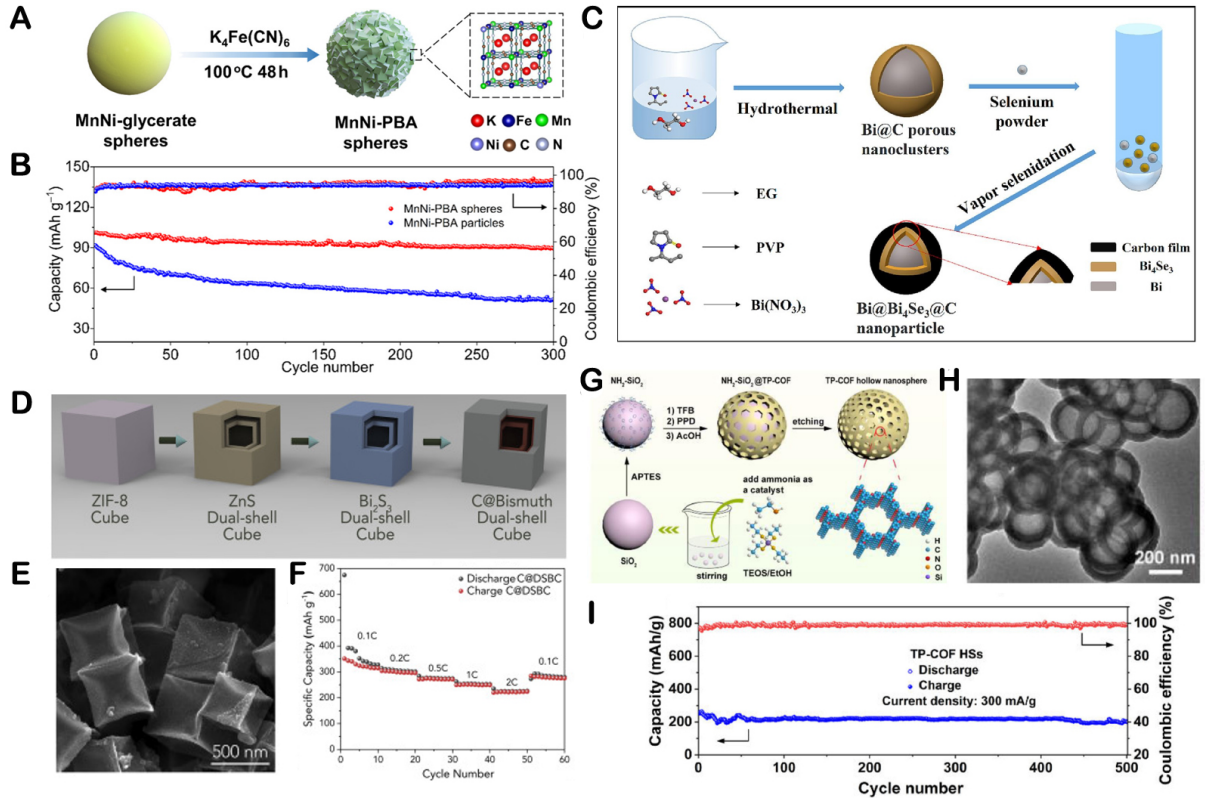

Figure 2. (A) Schematic illustration of the formation procedure of MnNi-PBA spheres. (B) Cycling performance of MnNi-PBA spheres and MnNi-PBA particles at 50 $mA \cdot g^{-1}$ (reprinted with permission[53]). (C) Schematic illustration of the procedure for the synthesis of the $Bi@Bi_4Se_3@C$ sample (reprinted with permission[55]). (D) Scheme illustrating the synthetic procedure of C@DSBC. (E) SEM image and (F) rate performance of C@DSBC (reprinted with permission[56]). (G) Schematic illustration of template-COF HSs. (H) TEM image and (I) prolonged cycling stability of TP-COF HSs (reprinted with permission[58]).

MOFs are one of the best examples because their modular nature offers great synthetic tunability and allows fine chemical and structural control. With creative synthetic design, properties such as porosity, stability, particle morphology, and conductivity can be tailored for specific applications. Designing heterostructures via a simple MOF-derived structure-inheritance strategy is an interesting approach. Bi/Bi_2O_3-C heterostructures designed using this approach facilitate interfacial charge transfer and alleviate the volume expansion of Bi/Bi_2O_3 during potassiation[57]. Recently introduced novel materials, such as imine-based covalent organic framework (COF) hollow nanospheres (TP-COF HSs), were designed using the same procedure and are capable of excellent K^+ storage owing to higher exposed active sites and wettability [Figure 2G-I][58].

Meeting the increased energy demand without increasing CO_2 emissions remains a major challenge. Bearing this in mind, several research groups have lately focused on developing bio-derived and bio-inspired energy devices [Figure 3][59].

The convergence of biological and synthetic materials is a disruptive area of study that presents considerable potential for developing bionic hybrid materials with improved properties, particularly with regard to energy storage. For instance, bio-derived materials (see Section "CONCLUSION AND FUTURE PERSPECTIVES"), such as biomass derived from potatoes, fungi, bacteria, dandelion seeds, cocoon-silk, and corn husk, have been employed as raw materials to synthesise porous carbon for use as anodes in PIBs.

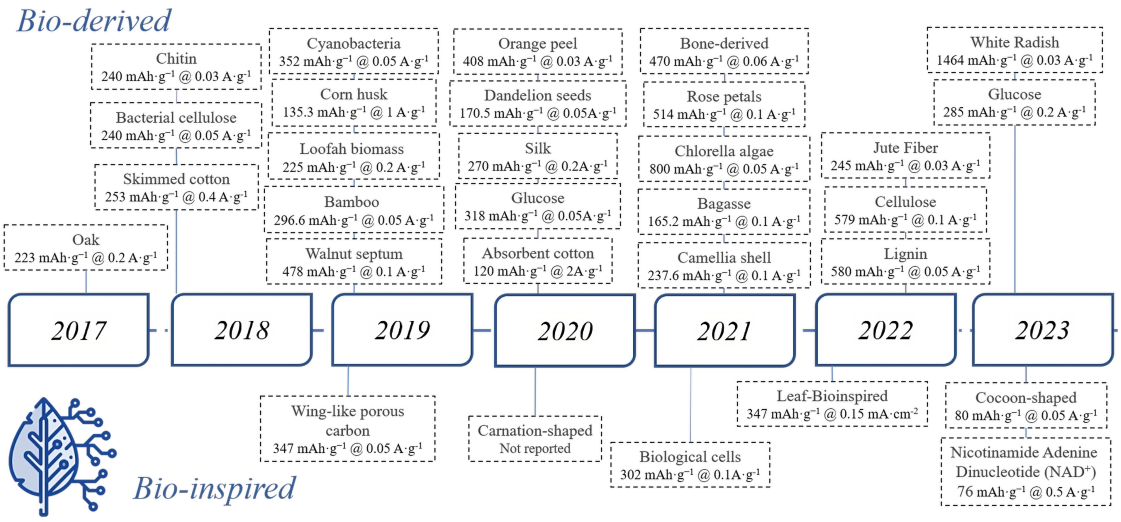

Figure 3. Timeline of the development of bio-derived (top) and bio-inspired (bottom) materials for PIBs (reprinted with permission[59]).

These materials act as a natural source of nitrogen/carbon and provide a bionic nanofiber network structural skeleton, thereby offering additional pathways that lead to the high-rate ion transport of K^+. Furthermore, bio-inspired materials can mimic the mechanism that nature has perfected over millions of years of evolution to generate and store energy directly. Some examples include the synthesis and functionalisation of bio-inspired hierarchical structures, achieved by the high integration degree of functionalities, with only basic construction materials[46]. Nevertheless, certain limitations need to be considered while attempting to meet the large-scale demand. For instance, some bio-derived materials often rely on specific feedstock sources, such as plants or microorganisms, whose availability may be limited or may require specific growth conditions. Moreover, the growth stages of bio-derived materials often influence their composition and performance. This variability poses difficulties in achieving consistent and standardised material properties, which is crucial for certain applications. Regarding bio-inspired materials, their functionality is derived from complex hierarchical structures. Precisely replicating these structures at a large scale can be technically challenging and also expensive. Sophisticated fabrication techniques or specialised equipment may be required, which limits the widespread adoption of such materials[60].

For example, Cui *et al.* utilised bio-inspired mineralisation (BM) to synthesise nanomaterials with controlled size, shape and polymorphs under freezing conditions to prepare anode materials for PIBs [Figure 4A-D][61]. Specifically, the feather-like sophisticated hierarchical structure obtained from methyl cellulose (MC)/$NaHCO_3$ flake precursors possessed a reversible capacity of 347 $mAh·g^{-1}$ at 50 $mA·g^{-1}$ and a relatively stable cyclability for 3,000 cycles. Wang *et al.* reported the rational design of four-electron accepting bithiophene-bridged carbonylpyridinium species [Figure 4E-G][62]. This design was inspired by the nicotinamide adenine dinucleotide in the respiratory chain. The non-conjugated polymers exhibited electrochemical activity and an effective ability to suppress dissolution in LIBs and NIBs. These polymers had a charge capacity of 331 $mAh·g^{-1}$, and the capacity retention was only 27% after 100 cycles in PIBs. The researchers attributed this result to the sluggish diffusion kinetics compared with Li^+ and Na^+ because of the larger ionic ratio that results in a Warburg factor of 91.7 (e.g., 41.8 for NIBs, which denotes faster ion diffusion). Another interesting study proposed a promising pathway for intelligent biomimetic electrodes to overcome the dissolution and shuttle issues faced by high-capacity electrodes in K-S batteries[63]. Specifically, the concept of intelligent nanofluidics was introduced in electrodes, and a leaf-bio-inspired electrode (Bio-CL@CoS_2/C) was proposed to solve these issues. The results showed that Bio-CL@CoS_2/C had obvious

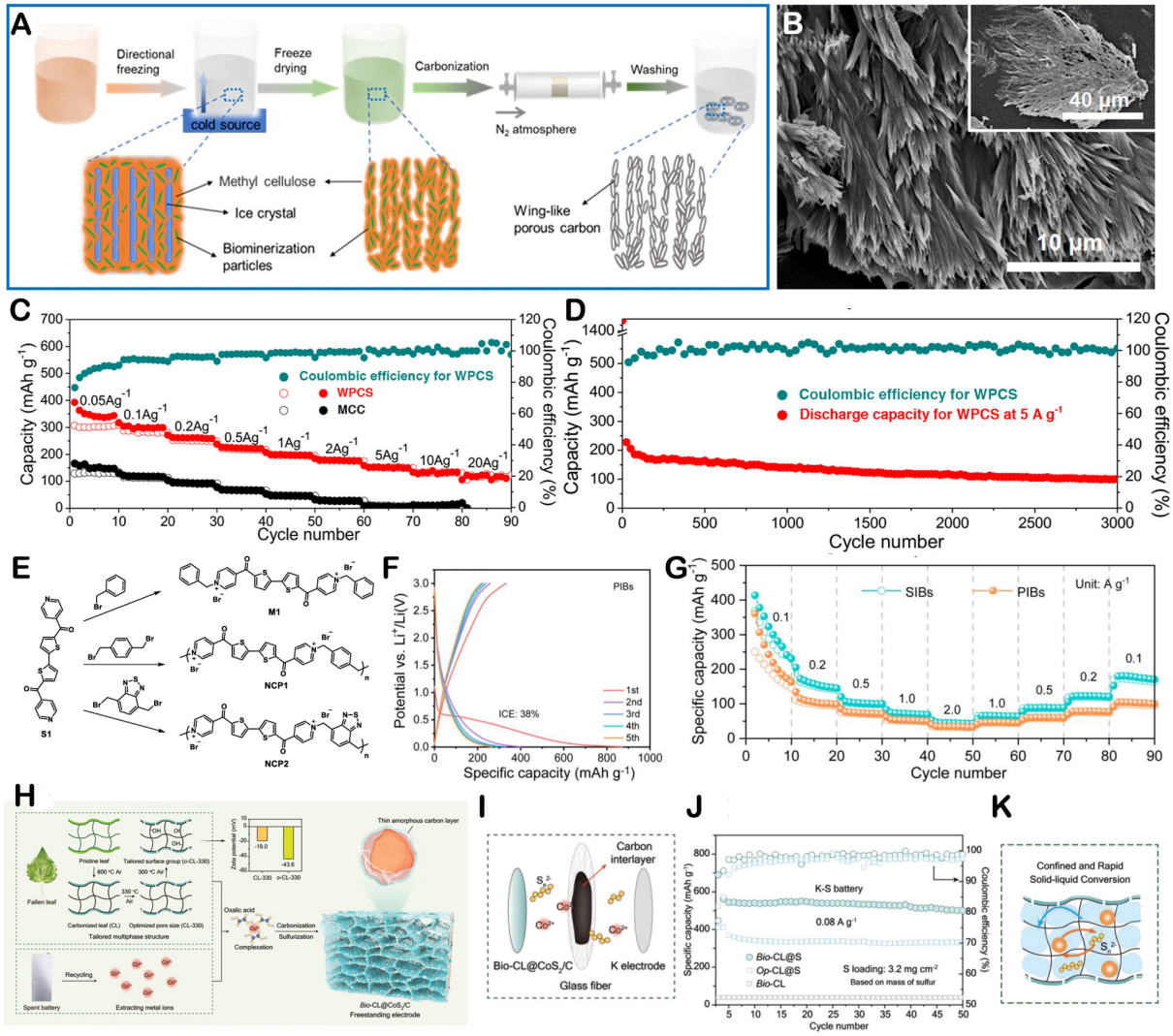

Figure 4. (A) Schematic diagram and (B) SEM image of the $NaHCO_3$ crystal coated with MCs using a directional freeze-drying process without carbonisation. (C) Rate capability profiles of WPCS and MCC electrodes. (D) Cycling performance at a current density of 5 $A{\cdot}g^{-1}$ (reprinted with permission[61]). (E) Synthesis route of non-conjugated poly(carbonylpyridinium)s (NCP1 and NCP2). (F) Galvanostatic charge/discharge curves of NCP2 electrode at 0.1 $A{\cdot}g^{-1}$. (G) Rate performance of NCP2 for NIBs and PIBs at different current densities (reprinted with permission[62]). (H) Schematic illustration of the synthesis process and (I) the carbon interlayer on the separator to capture shuttled species. (J) K-S battery system in the voltage range of 0.5-3.0 V. (K) Schematic illustration of efficient and self-protectable functions of this leaf-bio-inspired structure (reprinted with permission[63]).

advantages in increasing the areal capacity of the electrode and the rate capability (0.15% capacity decay per cycle) of metal sulphides [Figure 4H-K].

Regarding bio-inspired cathode materials for PIBs, not much information is available compared with Li or Na technology. Nevertheless, approaches such as the use of self-healing materials or the modification of the cathode chemical composition have been used to stabilise the cathode architecture during K^+ intercalation and deintercalation and avoid the detrimental effect of volume expansion. A study has recently proved that a cocoon-like structure, such as P3-type $K_{0.5}Mn_{0.7}Ni_{0.3}O_2$ (KMNO) [Figure 5A-C], enhances the structural stability with just 1.46% of volume exchange, thereby leading to a remarkable cycling stability of 77.0% over 300 cycles at 100 $mA{\cdot}g^{-1}$[64].

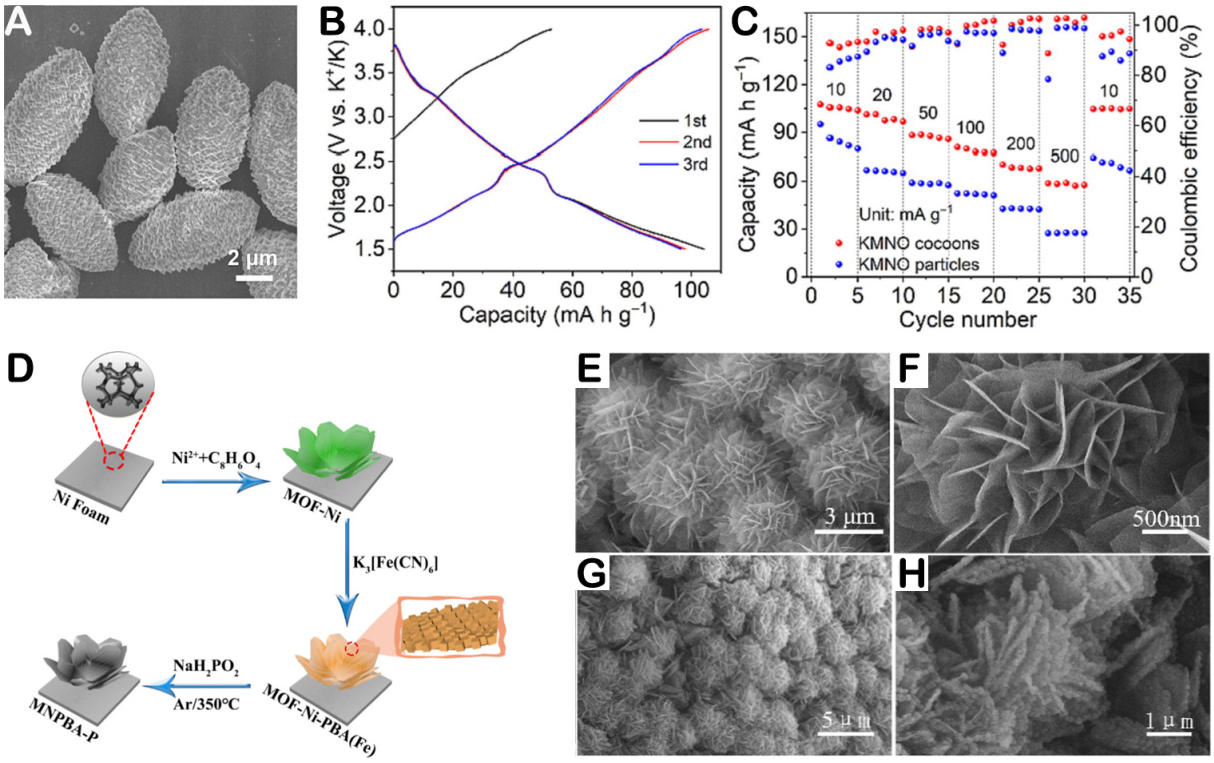

Figure 5. (A) SEM images of $Mn_{0.7}Ni_{0.3}CO_3$. (B) Galvanostatic charge/discharge curves at 20 mA·g^{-1} of KMNO cocoons. (C) Rate properties of the KMNO cocoons and KMNO particles and the corresponding Coulombic efficiencies (reprinted with permission[64]). (D) Schematic of the synthesis of the MNPBA-P grown on Ni foam. SEM images of (E and F) MOF-Ni and (G and H) MNPBA (reprinted with permission[65]).

As mentioned above [Figure 2A], Mn-Ni PBA spheres offered excellent capacity retention and good cycle life mainly because of the presence of Ni and the porous structure. Hence, it would be an interesting idea to grow Ni-Fe PBA on a carnation-shaped MOF-Ni. This strategy has been used by Xu *et al.* to develop a bifunctional electrocatalyst (MNPBA-P) for urea electrolysis [Figure 5D-H][65]. The high specific surface area, together with the good stability provided by the MOF structure, could make it an excellent candidate for application as a cathode material. In addition, MOFs can be tuned with different functionalities, which, together with the possibility of modifying the morphology, may augment their performance.

SELF-HEALING MATERIALS

Owing to the substantial volume changes occurring at the electrodes (~600%), mostly within the potassium particles, the interparticle contact and pulverisation decrease, which is accentuated during battery operation. Thus, the disintegration of particles and the lack of contact among them are responsible for considerable irreversible capacity loss and poor cycling stability in PIBs[66,67]. As previously mentioned, to enhance the cycle life of devices, electrode damage should be mitigated by developing new composite materials, and battery structural designs must also be optimised[60].

Additionally, self-healing materials that are able to identify, heal, and repair internal or external battery damage could become a reality in the near future. These self-healing mechanisms can be categorised as extrinsic and intrinsic. The former involves the incorporation of microencapsulated agents and micro-hollow fibres healing at the molecular level, and the latter involves the formation of reversible covalent and non-covalent bonds (e.g., covalent bonds formed via condensation, exchange or addition reactions, and

non-covalent bonds, such as hydrogen bonding and electrostatic, π-π, dipole-dipole, or host-guest interaction)[68,69]. Although few studies have been conducted on PIBs, most of the developments already realised for LIBs and NIBs could easily be applied to PIBs[70,71]. Scheme 1 summarises the different approaches and self-healing mechanisms reported for PIBs.

The use of self-healing materials has been focused on the electrolyte/anode interface by minimising the dendrite growth and reducing the anode disintegration by volume expansion. For example, materials that exhibit excellent deformability and, at the same time, are able to return to their original shape after cycling are of immense potential in potassium-based battery systems[72]. Cu_3BiS_3 anode exhibits phase and morphological reversibility, showing ultra-stable cycling performance (58% capacity retention after 12,000 cycles). This performance can be attributed to the self-healing mechanism that involves several steps. First, during an initial battery discharge to 0.01 V, the nanoparticles are transformed into small-grained intermediates comprising Cu, K_3Bi, and K_2S. Next, charging the battery up to 1.6 V leads to the formation of a Cu/Bi heterostructure interface that suppresses the shuttle effect (because Cu prevents the aggregation of Bi particles). Finally, during the charge process of up to 3 V, the small-grained intermediates are transformed back to the initial large-grained Cu_3BiS_3 nanoparticles. In self-healing materials, the concept of electrochemical reconstruction can reduce the capacity decay rate, improve the reactivity of the electrode, and maintain cycling stability.

Moreover, to overcome the volume expansion observed in intercalated graphite (KC_8) anodes while maintaining the theoretical capacitance (279 $mAh{\cdot}g^{-1}$), silicon carbide (SiC) has been proposed as an excellent candidate. Manju *et al.* performed first-principles density functional theory computations to assess the potential application of a monolayer SiC with the presence of vacancy and Stone-Wales type topological defects[73]. The authors suggested that the formation of stable 5-8-5 rings healing the vacancy created a transition from a point defect to a topological defect in the case of C-bivacancy and Si-C-bivacancy. As a result, negative binding energy, high specific capacity (501 $mAh{\cdot}g^{-1}$), low open circuit voltage (0.1 V), and low diffusion barrier (~0.77 eV) were obtained in LIBs. When a similar concept was applied to PIBs, a maximum capacity of 284.8 $mAh{\cdot}g^{-1}$ at a current density of 0.1 $A{\cdot}g^{-1}$ after 200 cycles and a highly reversible capacity of 197.3 $mAh{\cdot}g^{-1}$ at 1.0 $A{\cdot}g^{-1}$ after 1,000 cycles were observed.

In the specific case of the interface between the electrolyte (solid or liquid state) and the anode, self-healing binders and liquid metal materials are generally considered. In the case of self-healing binders, the focus is to avoid the disintegration of the anode because of volume changes after cycling. Various self-healing polymer binders have been developed, such as polyacrylic acid, polyamide-imide ureido-pyrimidinone (UPy), poly (ether-thioureas), and polyethene glycol[68,74]. Liquid metals (e.g., NaK, gallium (Ga) and its additives, and amalgams) have been used as anodes or as self-healing elastic interfaces that suppress the growth of dendrites[75-78]. Compared with conventional anode materials, liquid metal materials are ideal self-healing candidates owing to their liquid state, self-healing ability, and surface tension. Regarding liquid metals, most of them are based on Ga and its derivates (Ga-Sn, Ga-Si, Ga-In, or $CuGaS_2$)[79,80]. For instance, Ga-Sn alloy anodes possessed an excellent ability to repair the mechanical cracks generated during the cycling process. Unfortunately, the limited material selection and applicability of these self-healing liquid metal anodes are detrimental to their practical application in metal batteries.

Bearing this in mind, different metal-based amalgams (such as Li, Na, K, Al, Zn, Mg, Ag, Au, and Sn) can be used to overcome the interfacial challenges owing to their superior wetting properties. This concept was studied by Lagrange *et al.* as early as in the 1980s[81]; Fan *et al.* researched further and reported that glass-phase solid-state electrolyte interfaces are formed as the result of using different metals-Hg (e.g., Li, Al, Mg,

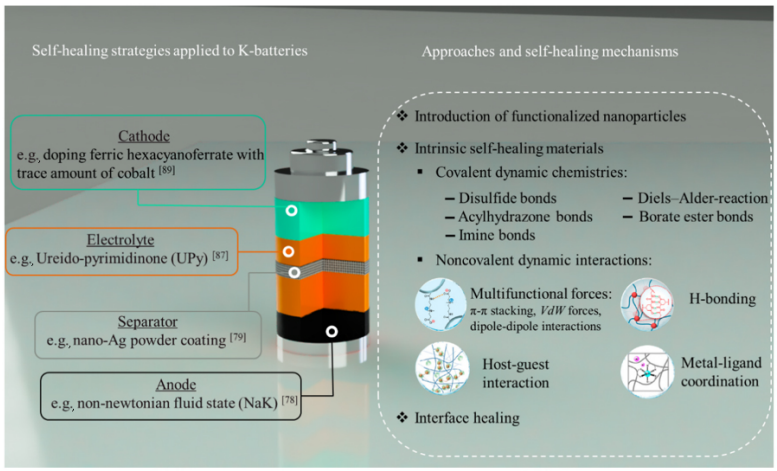

Scheme 1. Summary of the different approaches, self-healing mechanisms, and successful strategies applied in PIBs.

and Zn) and inorganic solid-state (Li_2S-P_2S_5)[75]. This leads to a long and stable cycling life, with only a small voltage hysteresis over hundreds of hours in a symmetric cell configuration.

Furthermore, the insertion of a fluid [namely, a liquid metal or a non-Newtonian fluid state (NaK)] in ordered structures (e.g., MOFs, COFs) offers new ways of achieving high-performance PIBs. In addition, the use of nanostructures has been examined as a strategy to enhance their long-term cycling, as these can prevent the strong adhesion and permeability observed in liquid anodes during battery operation. For this purpose, nano-Ag powder, a novel material, was synthesised recently as a functional anti-permeation film on the surface of the separator[76]. As a result, lower overpotential and higher specific capacity and Coulomb efficiency were attained in stretchable potassium-based batteries.

Several reviews have focused on the use of self-healing materials as electrolytes by adopting different strategies and employing various materials. Although only a few of them have been focused on PIBs, the topic is well covered[71,82]. It is important to highlight that these self-healing approaches can be extended to PIBs not only to improve their performance but also to comprehend the degradation kinetics and mechanisms that are dependent on several intrinsic and environmental conditions. To highlight one of the different materials, supramolecular polymers are designed using a polymer backbone [Figure 6][83-85] and multiple hydrogen-bonding UPy grafts. These polymers exhibit efficient self-healing, rapid shape-memory abilities and highly tunable mechanical properties owing to the dynamic supramolecular interactions.

The optimisation and operating mechanisms of cathode materials are paramount for reaching a satisfactory energy density of PIBs, as in the case of Li and Na batteries. Of the various cathode materials mentioned in the introduction section, PBAs are the most widely used ones owing to their facile preparation and high energy output. However, the charging and discharging processes can affect the properties of the electroactive materials in the battery. Recently, Xie *et al.* presented an innovative approach that involves the selective doping of ferric hexacyanoferrate (FeHCF) with trace amounts of Co to overcome the progressive degradation resulting from the self-healing mechanism of "electrochemically driven dissolution-recrystallization"[86]. As depicted in Figure 7, reversible recrystallisation is controlled by the electric field. The anchoring effect of Co to Fe crystalline sites effectively enhances the electric and ionic transportation properties, which facilitates self-healing characteristics (with an average Coulombic efficiency of 99.8% after 4,000 cycles) and superior electrochemical performance.

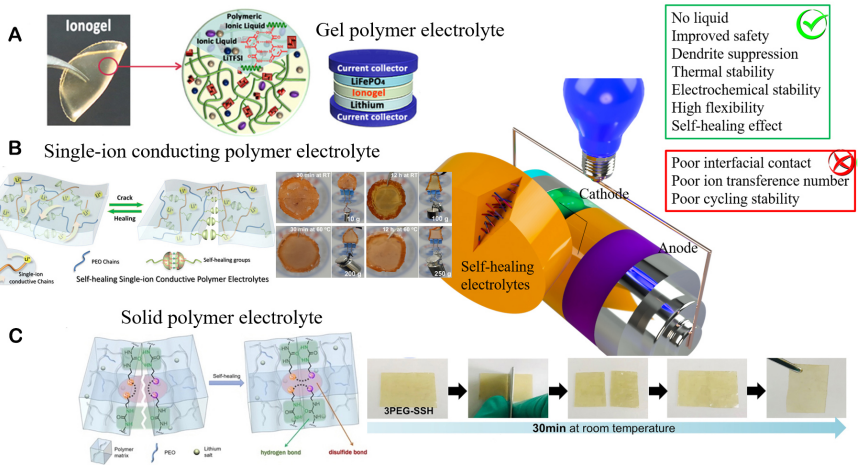

Figure 6. Pros and cons of self-healing polymer electrolytes for safer LIBs: examples of different categories explored so far. (A) Gel polymer electrolytes using an ionic liquid plasticiser demonstrating good flexibility and self-healing behaviour of the ionogel membrane based on a hydrogen-bonded supramolecular copolymer network when cut and placed inside a Li/$LiFePO_4$ button cell (reprinted with permission[83]). (B) Single ion conductive polymer electrolyte combining a lithium 4-styrenesulfonyl(phenylsulfonyl) imide (SSPSILi) unit for high Li-ion transference numbers and a quadrupole hydrogen bonding UPyMA unit for self-healing under different thermal and mechanical conditions, as shown in the optical images (reprinted with permission[84]). (C) Solid polymer electrolyte with self-healing capabilities enabled by dynamic disulfide and hydrogen-bonded polymer cross-links (reprinted with permission[85]).

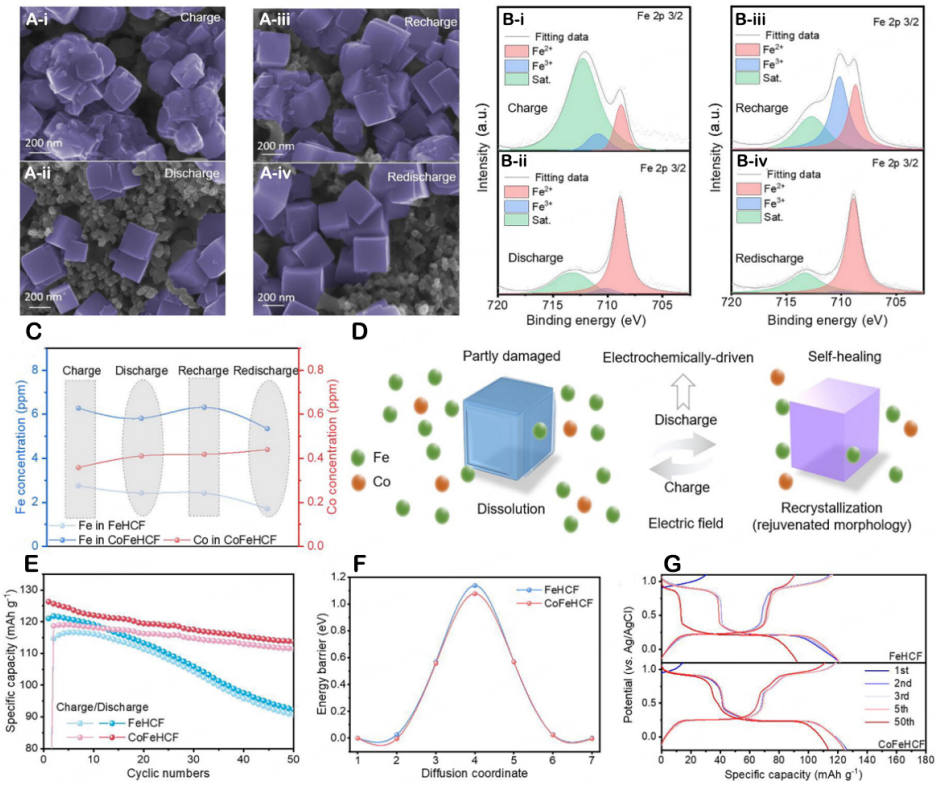

Figure 7. Effect of self-healing on the CoFeHCF electrode and electrolyte. SEM images (A) and XPS spectra (B) of CoFeHCF at selected charge/discharge states. (C) concentration variations of Fe and Co in electrolytes for the CoFeHCF electrode at the 21st and 22nd cycles. (D) a schematic of the "electrochemically driven dissolution-recrystallisation process". (E) the energy barrier for the diffusion of the potassium ion in CoFeHCF and the model for the migration pathways in the crystal model. (F) a comparison of the cycling performance at 0.1 $A{\cdot}g^{-1}$ between the two samples and (G) selected discharge/charge profiles of CoFeHCF and FeHCF (reprinted with permission[86]).

There is a need for new-generation materials that can augment the performance of PIB technologies that are currently in their infancy. Self-healing effects can also be obtained using the so-called "high energy conditions", such as temperature (e.g., ~60 °C) and high current density (e.g., 2 $mA \cdot cm^{-1}$). Li *et al*. examined this phenomenon in three different metal anodes (e.g., Li, Na, and K), with potassium dendrites exhibiting the highest self-healing ability and reparability under these conditions[87]. This effect has also been observed theoretically using a phase-field model with atom diffusion and heat transfer modules[79]. The researchers predicted that dendrites achieve thermal self-healing at ~55 °C via atom diffusion.

Recycled/sustainable materials

The application of sustainable functional materials in PIB technology not only relies on the use of highly abundant redox-active metal centres (such as Fe or Mn) or metal-free organic-based compounds but also encompasses the use of recycled materials from waste sources. With the PIB technology still in its infancy, there is ample opportunity to develop new resource-sustainable and environmentally friendly manufacturing chains. Furthermore, the incorporation of recycled and sustainable materials into the manufacturing of PIBs can contribute towards the ultimate goal of achieving truly circular economy ecosystems and also Sustainable Development Goal 7: Affordable and Clean Energy. Designing new manufacturing processes and industries within the scope of the circular economy paradigm is key to their long-term sustainability as it maintains materials and resources in use as long as possible. Consequently, new regulations are being enforced, such as the mandate within the European Union (EU) Circular Economy Plan on the Green Deal. This mandate sets minimum levels of used and recycled materials and collection targets for batteries produced in the EU[88-90]. In addition, car manufacturers are leaning towards the increased incorporation of recycled materials in their batteries instead of sourcing them from mining activities[91].

Estimates predict that spent end-of-life LIBs from electric vehicles alone would reach nearly four million tonnes annually by 2040[92]. The PIB manufacturing chain can take advantage of the surplus availability of used LIBs and make use of materials from secondary sources to ensure the sustainable manufacturing of PIBs. This topic has been explored by the PIB research community, albeit in a limited manner.

Recycled graphite from spent LIBs has been successfully employed as an anode material in PIBs, as reported in a study by Liang *et al*., where a high reversible capacity of 320 $mAh \cdot g^{-1}$ was achieved[93]. Employing a similar methodology, the back-integration of recovered graphite from waste batteries has been demonstrated [Figure 8]. In this case, the recycled graphite achieved a capacity of 361.4 $mAh \cdot g^{-1}$, with good cycling performance over 290 cycles[94].

Cathode materials for PIBs have also been produced by recycling waste materials. For instance, the team led by Zhu reported the transformation of rusty stainless-steel meshes into stable, low-cost, and binder-free cathodes[95]. The resulting Prussian blue-based cathode materials possessed a high capacity of 96.8 $mAh \cdot g^{-1}$, with a discharge voltage of 3.3 V and a high-rate capability. The materials retained 42% of their capacity at 1,000 $mA \cdot g^{-1}$ owing to the high electrical conductivity of the prepared system. Moreover, the cathode material exhibited commendable cycle stability, retaining 75.1% of the initial capacity after 305 cycles.

Recycled cathode components from LIBs have also been explored as anode materials. A recent study examined the successful transformation of spent $LiCoO_2$ into a $CoO/CoFe_2O_4$/graphite composite anode material[96]. The conversion of cathode materials into anode materials opens additional pathways that could be incorporated into the manufacturing of conversion anodes for PIBs.

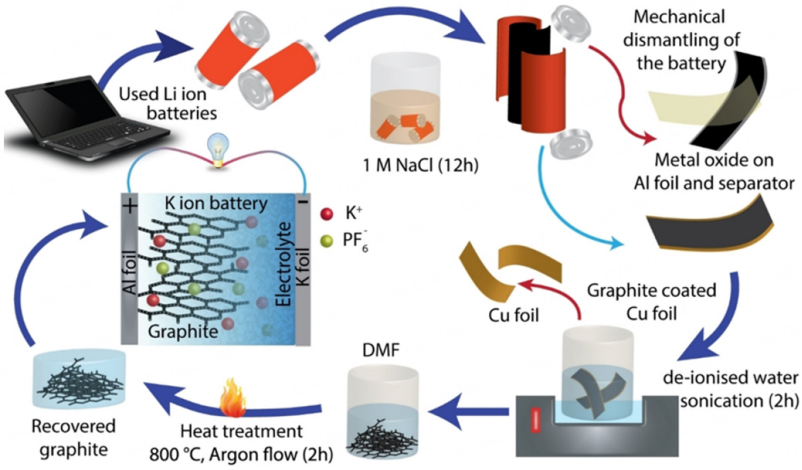

Figure 8. Schematic illustration of the recycling of graphite from spent LIBs and repurposing it as a potential electrode material in PIBs (reprinted with permission[94]).

The use of biomass sources to produce carbonaceous materials is a sustainable approach that has been widely explored. These represent an environmentally friendly and reasonably inexpensive source of carbon[97]. Furthermore, the use of biomass and carbon materials can produce tailored structures with customised porosity and high surface areas and materials with abundant functional groups [Figure 9][98-100]. The versatility of different biomass sources and preparation methods allows the synthesis of hard carbons from 0D to 3D entities, which can result in different anode cycling mechanisms. Most of the common cycling mechanisms are based on the intercalation-adsorption mechanism. These can be tuned by modifying the dimensionality of the structure to obtain targeted performance. Higher ion adsorption on the carbon surface permits higher cycling rates. Nevertheless, it can increase the overpotential between the charge and discharge processes. On the contrary, designing structures that promote intercalation mechanisms can result in lower intercalation voltages and, in turn, enhance energy efficiency. For example, in-depth studies on hard carbons from the *Magnolia grandiflora* Lima leaf revealed that the higher potential slope region is linked to the adsorption/desorption mechanism on the surface-active sites. The low-potential quasi-plateau region corresponds to the ion insertion/extraction in the graphitic-type interlayer[101]. The pyrolysis temperature affects the graphitisation level of the resulting carbonaceous electrode. In general, a lower carbonisation temperature can decrease the graphitisation of the material, thereby resulting in higher anode voltages. The use of a higher pyrolysis temperature, however, can reduce the available specific surface area of the material and the reactive sites. Moreover, the interlayer spacing is decreased, which is not conducive for the rapid insertion/extraction of K ions[102-104]. Thus, a rational study of the various pyrolysis treatments to produce different biomass-sourced carbon electrodes is required to fathom the interplay among material dimensionality, doping and active surface area and their relationship with the performance. A wide range of biomass products has been explored as carbonaceous electrode precursors for K-ion batteries. These include the use of different husks, dandelion seeds, walnuts, orange peels, bones, and seafoods[97]. Table 2 summarises the electrochemical performances of various carbonaceous PIB anode electrodes sourced from biomass.

The process of converting biomass material into carbonaceous anode materials depends on the slow pyrolysis of materials at temperatures > 400 °C in oxygen-free conditions to induce carbonisation[133]. Biomass-derived materials are usually subjected to acid activation to form highly porous structures, thereby increasing the surface area and improving the potassium-ion storage[103]. Some of these materials have achieved outstanding high-performance metrics. This is the case of nitrogen-rich hard carbons obtained

Table 2. Summary of various biomass-sourced carbonaceous anode materials and their electrochemical performance in potassium half-cells (adapted and updated from Yuan *et al.*[97])

Anode materials	Morphology	SSA ($m^2 \cdot g^{-1}$)	Electrolyte system	Initial Capacity ($mAh \cdot g^{-1}$)	Voltage window (V)	Capacity retention ($mAh \cdot g^{-1}$)	Highest rate performance ($mAh \cdot g^{-1}$)	References
Chitin	Fibre	309.45	KPF_6 in EC/DEC	240 at 28 $mA \cdot g^{-1}$	0.01-2.0	215 after 200 cycles at 6 $mA \cdot g^{-1}$	103.4 at 0.56 $A \cdot g^{-1}$	[105]
Bacterial cellulose	Fibre	778.75	KPF_6 in EC/DEC	240 at 50 $mA \cdot g^{-1}$	0.01-2.8	158 after 2,000 cycles at 1 $A \cdot g^{-1}$	122 at 5 $A \cdot g^{-1}$	[106]
Potato	Irregular	531.67	KFSI in DME	248 at 100 $mA \cdot g^{-1}$	0.01-2.7	171 after 400 cycles at 0.5 $A \cdot g^{-1}$	152 at 1 $A \cdot g^{-1}$	[107]
Loofah	Fibre	270	KPF_6 in EC/DEC	155 at 100 $mA \cdot g^{-1}$	0.01-3.0	~150 after 200 cycles at 0.1 $A \cdot g^{-1}$	70 at 0.2 $A \cdot g^{-1}$	[108]
Cyanobacteria	Network	473.7	KPF_6 in EC/DEC	352 at 50 $mA \cdot g^{-1}$	0.01-3.0	266 after 100 cycles at 0.05$A \cdot g^{-1}$	155 at 1 $A \cdot g^{-1}$	[109]
Maple leaves	Irregular	62.6	$KClO_4$ in EC/DEC	359 at 50 $mA \cdot g^{-1}$	0.01-3.0	141.9 after 1,000 cycles at 1 $A \cdot g^{-1}$	144.8 at 1 $A \cdot g^{-1}$	[110]
Skimmed cotton	Fibre	612	KPF_6 in DME	409 at 100 $mA \cdot g^{-1}$	0.01-2.0	120 after 500 cycles at 2 $A \cdot g^{-1}$	135 at 2 $A \cdot g^{-1}$	[111]
Sugar cane	Bowl	425.1	KPF_6 in EC/DEC	463 at 100 $mA \cdot g^{-1}$	0.01-2.5	304 after 150 cycles at 0.1 $A \cdot g^{-1}$	182 at 2 $A \cdot g^{-1}$	[112]
Oak	Irregular	156	KPF_6 in EC/DEC	233 at 20 $mA \cdot g^{-1}$	0.01-2.3	~140 after 150 cycles at 0.1 $A \cdot g^{-1}$	135 at 0.1 $A \cdot g^{-1}$	[113]
Skimmed cotton	Fibre	354	KPF_6 in DME	253 at 40 $mA \cdot g^{-1}$	0.01-2.0	240 after 150 cycles at 0.2 $A \cdot g^{-1}$	165 at 4 $A \cdot g^{-1}$	[114]
Artemisia hedinii	Irregular	1196	KPF_6 in EC/DEC	116 at 70 $mA \cdot g^{-1}$	0.01-3.0	110 after 500 cycles at 0.07 Ag^{-1}	~115 at 0.14 $A \cdot g^{-1}$	[115]
Walnut septum	Open hierarchical tubular porous	99.6	KPF_6 in EC/DEC	478 at 100 $mA \cdot g^{-1}$	0.005-3.0	120 after 1,000 cycles at 1 $A \cdot g^{-1}$	102.6 at 2 $A \cdot g^{-1}$	[116]
Corn husk	Hierarchical porous structure	3.4	KPF_6 in EC/DEC	396 at 100 $mA \cdot g^{-1}$	0.005-3.0	135 after 500 cycles at 1 $A \cdot g^{-1}$	167 at 2 $A \cdot g^{-1}$	[117]
Dandelion seeds	Irregular	1303	KPF_6 in EC/DEC	168 at 50 $mA \cdot g^{-1}$	0.01-2.0	170 after 100 cycles at 0.05 $A \cdot g^{-1}$	49 at 1 $A \cdot g^{-1}$	[118]
Seafood waste (Chitin)	Microspheres	563	KPF_6 in EC/DEC	~320 at 35 $mA \cdot g^{-1}$	0.01-3.0	180 after 4,000 at 0.5 $A \cdot g^{-1}$	154 at 2 $A \cdot g^{-1}$	[99]
White radish	Irregular	412.8	KPF_6 in EC/DEC	1,464 at 25 $mA \cdot g^{-1}$	0.01-2.5	410 after 150 cycles at 0.025 $A \cdot g^{-1}$	98 at 1 $A \cdot g^{-1}$	[100]
Jute fiber	Fibre	210.9	KPF_6 in EC/DEC	245 at 30 $mA \cdot g^{-1}$	0.005-1.5	194 after 50 cycles at 0.03 $A \cdot g^{-1}$	32 at 3 $A \cdot g^{-1}$	[119]
Bone-derived	Hierarchical porous structure	1474.5	KPF_6 in EC/DEC	470 at 58 $mA \cdot g^{-1}$	0.01-3.0	205 after 450 cycles at 0.06 $A \cdot g^{-1}$	113 at 0.58 $A \cdot g^{-1}$	[120]
Rose petals	Hemispherical micropillar	Not reported	KFSI in EC/DMC	514 at 100 $mA \cdot g^{-1}$	0.01-3.0	193 after 800 cycles at 0.5 $A \cdot g^{-1}$	134.6 at 1 $A \cdot g^{-1}$	[121]

Water chestnut	Irregular	106.5	KFSI in EC/DEC	~475 at 100 mA·g^{-1}	0.01-3.0	220 after 1,000 cycles at 0.1 A·g^{-1}	134.8 at 1 A·g^{-1}	[122]
Orange peel	Irregular	64.25	KPF_6 in EC/DMC	408 at 30 mA·g^{-1}	0.01-2.0	112 after 3,000 cycles at 0.5 A·g^{-1}	101.5 at 1 A·g^{-1}	[98]
Soybeans	Irregular	379.9	KPF_6 in EC/DEC	543 at 50 mA·g^{-1}	0.01-3.0	200 after 900 cycles at 0.05 A·g^{-1}	70 at 0.8 A·g^{-1}	[123]
Cocoon silk	Irregular	977.7	KFSI in EC/DMC	~390 at 25 mA·g^{-1}	0.01-3.0	270 after 923 cycles at 0.2 A·g^{-1}	164 at 1 A·g^{-1}	[124]
Ganoderma lucidum spore	Cage	104	KPF_6 in EC/DEC	823 at 50 mA·g^{-1}	0.02-3.0	125 after 700 cycles at 1 A·g^{-1}	133 at 1 A·g^{-1}	[125]
Bamboo	Rod-like fibre	336.4	KPF_6 in EC/DEC	339 at 50 mA·g^{-1}	0.01-3.0	204 after 300 cycles at 0.2 A·g^{-1}	124.2 at 1 A·g^{-1}	[126]
Glucose	Irregular	280.0	KFSI in EC/DMC	~285 at 200 mA·g^{-1}	0.01-3.0	148 after 950 cycles at 0.2 A·g^{-1}	100 at 5 A·g^{-1}	[127]
Chlorella pyrenoidosa algae	Fibre	Not reported	KFSI in DME	~800 at 50 mA·g^{-1}	0.01-3.0	207 after 800 cycles at 2 A·g^{-1}	185 at 5 A·g^{-1}	[128]
Vitamin K	Irregular	Not reported	KPF_6 in EC/DEC	466 at 100 mA·g^{-1}	0.1-2.5	222 after 100 cycles at 0.1 A·g^{-1}	165 at 1 A·g^{-1}	[129]
Lignin	Irregular	6.1	KPF_6 in EC/DEC	~580 at 50 mA·g^{-1}	0.01-3.0	237 after 100 cycles at 0.05 A·g^{-1}	171 at 0.2 A·g^{-1}	[130]
Cellulose	Honeycomb-like surface	22	KFSI in DME/TFETFEE	579 at 100 mA·g^{-1}	0.01-3.8	203 after 6,000 cycles at 2 A·g^{-1}	121 at 10 A·g^{-1}	[131]
Rice husk	Irregular	365.4	KPF_6 in EC/DEC	~490 at 30 mA·g^{-1}	0.01-3.0	104 after 500 cycles at 0.5 A·g^{-1}	63 at 1 A·g^{-1}	[132]

from seafood waste chitin biomass, where an impressive rate performance of 154 mAh·g^{-1} at 20.2 A·g^{-1} and an ultralong cycle life of 4,000 cycles without any noticeable capacity decay have been reported[99]. Generally, the formation of hard carbons from biomass can produce high-performing anodes with a long cycling life comparable to those from synthetic hard carbons[44,134], thus representing a viable sustainable alternative for PIB anode materials.

Non-biomass waste has also been explored as a source of carbonaceous materials. In this regard, pyrolysis of sulfonated waste tire rubber into high value-added hard carbons has been reported, with a capacity of 220 mAh·g^{-1} at 28 mA·g^{-1}[135].

The use of biomass is not limited to the production of electrode materials, and solid electrolytes have also been produced from biomass. The use of lignin for the preparation of hard carbons has been reported[132], and recently, Trano *et al.* have explored its use as a precursor for the preparation of polymer electrolytes[136]. The lignin-based polymer presented ionic conductivity exceeding 10^{-3} S·cm^{-1} at ambient temperatures and a wide stability window of up to 4 V

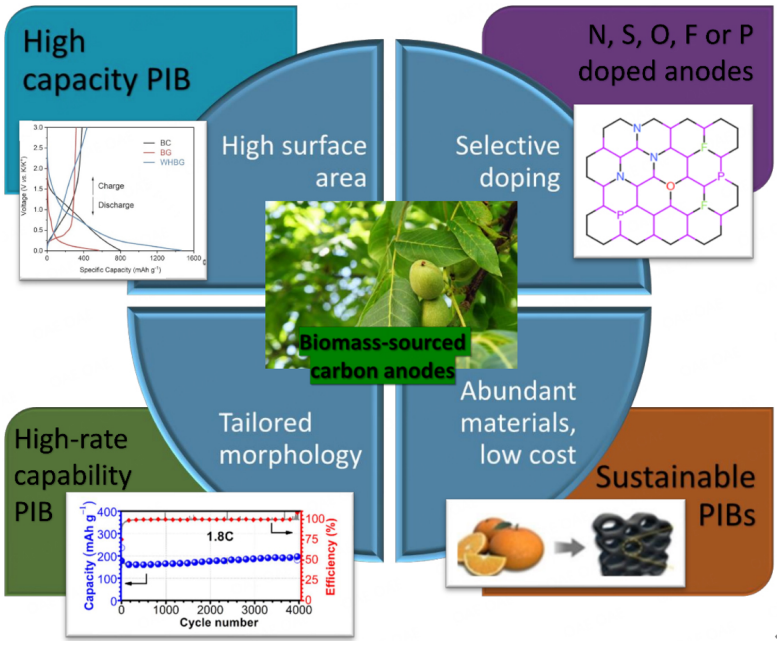

Figure 9. Schematic representation of the versatility of biomass-sourced carbon anodes as functional materials in PIBs (inset graphs reproduced with permission[98-100]).

vs. K^+/K. Furthermore, the use of cardanol as a precursor for producing epoxy resins as bio-based gel polymer electrolytes has been investigated. In this case, the electrolyte stability window was increased to 5 V *vs.* K^+/K while retaining the same level of ionic conductivity in the $mS \cdot cm^{-1}$ range[137].

The studies highlighted in this section demonstrate the enormous possibilities for developing sustainable and environmentally friendly pathways for exploiting PIB technology.

CONCLUSION AND FUTURE PERSPECTIVES

Although PIBs are considered promising low-cost candidates for large-scale energy storage applications by virtue of the abundant reserves of potassium resources, anode volume expansion and slow ion diffusion are the major bottlenecks in their commercialisation.

This review has focused on the use of advanced materials to overcome these issues. Specifically, bio-derived and bio-inspired materials have gained increasing attention over the last few years, taking advantage of structures present in nature. Moreover, to avoid structural anode degradation after cycling, materials with self-healing properties have been successfully incorporated into PIBs. This has reduced the overpotential and enhanced the specific capacity and cycling stability. However, issues related to processability and compatibility need to be considered for the successful application of self-healing materials in PIBs.

In addition, the selection of materials employed in new-generation energy storage devices requires consideration of additional key factors, such as the use of non-toxic and environment-friendly materials in the preparation process and the need to reduce energy consumption and waste generation. With the PIB technology still in its infancy, there is an immense opportunity to develop new resource-sustainable and environmentally friendly manufacturing chains. The incorporation of recycled and sustainable materials into the manufacturing of PIBs can aid in attaining the ultimate goal of truly circular economy ecosystems and further contribute to the realisation of sustainable development goals.

Motivated by the recent findings, this review has summarised the most relevant approaches to give shape to the idea of developing practical PIBs in terms of performance and sustainability. In particular, future developments are likely to focus on the development of self-bonding systems as intrinsic self-healing and stretchable multi-layered devices with robust interfaces and improved durability. The current advances in PIB research, such as self-healing materials, are opening novel avenues for advanced technologies with higher energy densities, such as solid-state or chalcogen-based chemistries. These technologies are presently being limited by the continuous degradation of the active components during battery operation.

DECLARATIONS

Authors' contributions

Writing - review and editing: Salado M, Amores M, Pozo-Gonzalo C, Lanceros-Méndez S, Forsyth M
Writing - original draft preparation: Salado M, Amores M
All authors have read and agreed to the published version of the manuscript.

Availability of data and materials

Not applicable.

Financial support and sponsorship

Salado M. acknowledges the funding from the European Union H2020 Program under the Marie Skłodowska Curie global fellowship (ROCHE, 101026163). This study is a part of the Advanced Materials program and was supported by MCIN with funding from European Union NextGenerationEU (PRTR-C17.I1) and by the Basque Government under the IKUR program.

Conflicts of interest

All authors declared that there are no conflicts of interest.

Ethics approval and consent to participate

Not applicable.

Consent for publication

Not applicable.

REFERENCES

1. Divakaran AM, Minakshi M, Bahri PA, et al. Rational design on materials for developing next generation lithium-ion secondary battery. *Prog Solid State Chem* 2021;62:100298. DOI
2. Dillard CD, Nevle EP. Supply chain disruptions in the energy industry: challenges with the supply of lithium-ion batteries. Foley & Lardner LLP. 2022. Available from: https://www.foley.com/en/insights/publications/2022/09/supply-chain-disruptions-energy-lithium-ion [Last accessed on 1 Aug 2023].
3. Tedesco M. The paradox of lithium. News from the Columbia Climate School. 2023. Available from: https://news.climate.columbia.edu/2023/01/18/the-paradox-of-lithium/ [Last accessed on 1 Aug 2023].
4. Vaalma C, Buchholz D, Weil M, Passerini S. A cost and resource analysis of sodium-ion batteries. *Nat Rev Mater* 2018;3:18013. DOI
5. Kubota K, Dahbi M, Hosaka T, Kumakura S, Komaba S. Towards K-ion and Na-ion batteries as "beyond Li-ion". *Chem Rec* 2018;18:459-79. DOI PubMed
6. Matsuda Y, Nakashima H, Morita M, Takasu Y. Behavior of some ions in mixed organic electrolytes of high energy density batteries.

J Electrochem Soc 1981;128:2552-6. DOI
7. Marcus Y. Transfer of ions between solvents: some new results concerning volumes, heat capacities and other quantities. *Pure Appl Chem* 1996;68:1495-500. DOI
8. Okoshi M, Yamada Y, Komaba S, Yamada A, Nakai H. Theoretical analysis of interactions between potassium ions and organic electrolyte solvents: a comparison with lithium, sodium, and magnesium ions. *J Electrochem Soc* 2017;164:A54-60. DOI
9. Xu Y, Ding T, Sun D, Ji X, Zhou X. Recent advances in electrolytes for potassium-ion batteries. *Adv Funct Mater* 2023;33:2211290. DOI
10. SMM - China metal market. 2023. Available from: https://www.metal.com/ [Last accessed on 1 Aug 2023].
11. Anoopkumar V, Bibin J, Mercy TD. Potassium-ion batteries: key to future large-scale energy storage? *ACS Appl Energy Mater* 2020;3:9478-92. DOI
12. Eftekhari A. On the theoretical capacity/energy of lithium batteries and their counterparts. *ACS Sustain Chem Eng* 2019;7:3684-7. DOI
13. Eftekhari A. Potassium secondary cell based on Prussian blue cathode. *J Power Sources* 2004;126:221-8. DOI
14. Jian Z, Luo W, Ji X. Carbon electrodes for K-ion batteries. *J Am Chem Soc* 2015;137:11566-9. DOI PubMed
15. Komaba S, Hasegawa T, Dahbi M, Kubota K. Potassium intercalation into graphite to realize high-voltage/high-power potassium-ion batteries and potassium-ion capacitors. *Electrochem Commun* 2015;60:172-5. DOI
16. Xue L, Li Y, Gao H, et al. Low-cost high-energy potassium cathode. *J Am Chem Soc* 2017;139:2164-7. DOI
17. Rajagopalan R, Tang Y, Ji X, Jia C, Wang H. Advancements and challenges in potassium ion batteries: a comprehensive review. *Adv Funct Mater* 2020;30:1909486. DOI
18. Hosaka T, Kubota K, Hameed AS, Komaba S. Research development on K-ion batteries. *Chem Rev* 2020;120:6358-466. DOI PubMed
19. Zhao S, Guo Z, Yan K, et al. The rise of Prussian blue analogs: challenges and opportunities for high-performance cathode materials in potassium-ion batteries. *Small Struct* 2021;2:2000054. DOI
20. Delmas C, Fouassier C, Hagenmuller P. Structural classification and properties of the layered oxides. *Physica B+C* 1980;99:81-5. DOI
21. Jo JH, Choi JU, Park YJ, et al. P2-$K_{0.75}[Ni_{1/3}Mn_{2/3}]O_2$ cathode material for high power and long life potassium-ion batteries. *Adv Energy Mater* 2020;10:1903605. DOI
22. Nathan MGT, Yu H, Kim GT, et al. Recent advances in layered metal-oxide cathodes for application in potassium-ion batteries. *Adv Sci* 2022;9:e2105882. DOI PubMed PMC
23. Hosaka T, Shimamura T, Kubota K, Komaba S. Polyanionic compounds for potassium-ion batteries. *Chem Rec* 2019;19:735-45. DOI PubMed
24. Recham N, Rousse G, Sougrati MT, et al. Preparation and characterization of a stable $FeSO_4$ F-based framework for alkali ion insertion electrodes. *Chem Mater* 2012;24:4363-70. DOI
25. Zhang W, Huang W, Zhang Q. Organic materials as electrodes in potassium-ion batteries. *Chemistry* 2021;27:6131-44. DOI PubMed
26. Ding J, Zhang H, Fan W, Zhong C, Hu W, Mitlin D. Review of emerging potassium-sulfur batteries. *Adv Mater* 2020;32:e1908007. DOI PubMed
27. Liu Q, Deng W, Pan Y, Sun CF. Approaching the voltage and energy density limits of potassium-selenium battery chemistry in a concentrated ether-based electrolyte. *Chem Sci* 2020;11:6045-52. DOI PubMed PMC
28. Wang X, Wang H. Designing carbon anodes for advanced potassium-ion batteries: materials, modifications, and mechanisms. *Adv Powder Mater* 2022;1:100057. DOI
29. Sha M, Liu L, Zhao H, Lei Y. Anode materials for potassium-ion batteries: current status and prospects. *Carbon Energy* 2020;2:350-69. DOI
30. Zhang W, Pang WK, Sencadas V, Guo Z. Understanding high-energy-density Sn_4P_3 anodes for potassium-ion batteries. *Joule* 2018;2:1534-47. DOI
31. Ni L, Xu G, Li C, Cui G. Electrolyte formulation strategies for potassium-based batteries. *Exploration* 2022;2:20210239. DOI PubMed PMC
32. Sun H, Liang P, Zhu G, et al. A high-performance potassium metal battery using safe ionic liquid electrolyte. *Proc Natl Acad Sci USA* 2020;117:27847-53. DOI PubMed PMC
33. Yoshii K, Masese T, Kato M, Kubota K, Senoh H, Shikano M. Sulfonylamide-based ionic liquids for high-voltage potassium-ion batteries with honeycomb layered cathode oxides. *ChemElectroChem* 2019;6:3901-10. DOI
34. Hosaka T, Kubota K, Kojima H, Komaba S. Highly concentrated electrolyte solutions for 4 V class potassium-ion batteries. *Chem Commun* 2018;54:8387-90. DOI PubMed
35. Touja J, Le Pham PN, Louvain N, Monconduit L, Stievano L. Effect of the electrolyte on K-metal batteries. *Chem Commun* 2020;56:14673-6. DOI PubMed
36. Zhang Q, Mao J, Pang WK, et al. Boosting the potassium storage performance of alloy-based anode materials via electrolyte salt chemistry. *Adv Energy Mater* 2018;8:1703288. DOI
37. Zhao J, Zou X, Zhu Y, Xu Y, Wang C. Electrochemical intercalation of potassium into graphite. *Adv Funct Mater* 2016;26:8103-10. DOI

38. Liu G, Cao Z, Zhou L, et al. Additives engineered nonflammable electrolyte for safer potassium ion batteries. *Adv Funct Mater* 2020;30:2001934. DOI
39. Tan H, Lin X. Electrolyte design strategies for non-aqueous high-voltage potassium-based batteries. *Molecules* 2023;28:823. DOI PubMed PMC
40. Zhao X, Lu Y, Qian Z, Wang R, Guo Z. Potassium-sulfur batteries: status and perspectives. *EcoMat* 2020;2:e12038. DOI
41. Suo G, Zhang J, Li D, et al. Flexible N doped carbon/bubble-like MoS_2 core/sheath framework: buffering volume expansion for potassium ion batteries. *J Colloid Interface Sci* 2020;566:427-33. DOI
42. Fei H, Liu Y, An Y, et al. Stable all-solid-state potassium battery operating at room temperature with a composite polymer electrolyte and a sustainable organic cathode. *J Power Sources* 2018;399:294-8. DOI
43. Zhang X, Meng J, Wang X, Xiao Z, Wu P, Mai L. Comprehensive insights into electrolytes and solid electrolyte interfaces in potassium-ion batteries. *Energy Stor Mater* 2021;38:30-49. DOI
44. Xu Y, Titirici M, Chen J, et al. 2023 roadmap for potassium-ion batteries. *J Phys Energy* 2023;5:021502. DOI
45. Narayan R, Laberty-robert C, Pelta J, Tarascon J, Dominko R. Self-healing: an emerging technology for next-generation smart batteries. *Adv Energy Mater* 2022;12:2102652. DOI
46. Mei J, Liao T, Peng H, Sun Z. Bioinspired materials for energy storage. *Small Methods* 2022;6:e2101076. DOI
47. Lu C, Chen X. Learn from nature: bio-inspired structure design for lithium-ion batteries. *EcoMat* 2022;4:e12181. DOI
48. Zhao Y, Ruether T, Bhatt AI, Staines J. Australian landscape for lithium ion battery recycling and reuse in 2020 - current status, gap analysis and industry perspectives. 2021. Available from: https://fbicrc.com.au/wp-content/uploads/2021/03/CSIRO-Report-Australian-landscape-for-lithium-ion-battery-recycling-and-reuse-in-2020.pdf [Last accessed on 1 Aug 2023].
49. Yu F, Li S, Chen W, Wu T, Peng C. Biomass-derived materials for electrochemical energy storage and conversion: overview and perspectives. *Energy Environ Mater* 2019;2:55-67. DOI
50. Hudak NS. 4 - Nanostructured electrode materials for lithium-ion batteries. In: lithium-ion batteries. Amsterdam, The Netherlands: Elsevier; 2014. pp. 57-82. DOI
51. Guari Y, Cahu M, Félix G, et al. Nanoheterostructures based on nanosized Prussian blue and its Analogues: design, properties and applications. *Coord Chem Rev* 2022;461:214497. DOI
52. Ming H, Torad NLK, Chiang Y, Wu KC, Yamauchi Y. Size- and shape-controlled synthesis of Prussian Blue nanoparticles by a polyvinylpyrrolidone-assisted crystallization process. *CrystEngComm* 2012;14:3387-96. DOI
53. Li A, Duan L, Liao J, Sun J, Man Y, Zhou X. Formation of Mn-Ni Prussian blue analogue spheres as a superior cathode material for potassium-ion batteries. *ACS Appl Energy Mater* 2022;5:11789-96. DOI
54. Nithya C, Modigunta JKR, In I, Kim S, Gopukumar S. Bi_2S_3 nanorods deposited on reduced graphene oxide for potassium-ion batteries. *ACS Appl Nano Mater* 2023;6:6121-32. DOI
55. Li Z, Yang J, Zhou Z, et al. Growth confinement and ion transportation acceleration via an in-situ formed Bi_4Se_3 layer for potassium ion battery anodes. *Appl Surf Sci* 2023;621:156785. DOI
56. Xie F, Zhang L, Chen B, et al. Revealing the origin of improved reversible capacity of dual-shell bismuth boxes anode for potassium-ion batteries. *Matter* 2019;1:1681-93. DOI
57. Zhang P, Wei Y, Zhou S, Soomro RA, Jiang M, Xu B. A metal-organic framework derived approach to fabricate in-situ carbon encapsulated Bi/Bi_2O_3 heterostructures as high-performance anodes for potassium ion batteries. *J Colloid Interface Sci* 2023;630:365-74. DOI
58. Sun J, Tian R, Man Y, Fei Y, Zhou X. Templated synthesis of imine-based covalent organic framework hollow nanospheres for stable potassium-ion batteries. *Chin Chem Lett* 2023;34:108233. DOI
59. Singh R, Rhee H. The rise of bio-inspired energy devices. *Energy Stor Mater* 2019;23:390-408. DOI
60. Mishra S, Yılmaz-serçinoğlu Z, Moradi H, Bhatt D, Kuru Cİ, Ulucan-karnak F. Recent advances in bioinspired sustainable sensing technologies. *Nano-Struct Nano-Objects* 2023;34:100974. DOI
61. Cui Y, Liu W, Wang X, et al. Bioinspired mineralization under freezing conditions: an approach to fabricate porous carbons with complicated architecture and superior K^+ storage performance. *ACS Nano* 2019;13:11582-92. DOI
62. Wang X, Chen L, He X. Bio-inspired non-conjugated poly(carbonylpyridinium) as anode material for high-performance alkali-ion (Li^+, Na^+, and K^+) batteries. *J Colloid Interface Sci* 2023;643:541-50. DOI
63. Zhang X, Wu F, Lv X, et al. Achieving sustainable and stable potassium-ion batteries by leaf-bioinspired nanofluidic flow. *Adv Mater* 2022;34:e2204370. DOI
64. Duan L, Xu J, Xu Y, et al. Cocoon-shaped P3-type $K_{0.5}Mn_{0.7}Ni_{0.3}O_2$ as an advanced cathode material for potassium-ion batteries. *J Energy Chem* 2023;76:332-8. DOI
65. Xu H, Ye K, Zhu K, et al. Transforming carnation-shaped MOF-Ni to Ni-Fe prussian blue analogue derived efficient bifunctional electrocatalyst for urea electrolysis. *ACS Sustain Chem Eng* 2020;8:16037-45. DOI
66. Popovic J. The importance of electrode interfaces and interphases for rechargeable metal batteries. *Nat Commun* 2021;12:6240. DOI PubMed PMC
67. Kim EJ, Kumar PR, Gossage ZT, et al. Active material and interphase structures governing performance in sodium and potassium ion batteries. *Chem Sci* 2022;13:6121-58. DOI PubMed PMC
68. Marinow A, Katcharava Z, Binder WH. Self-healing polymer electrolytes for next-generation lithium batteries. *Polymers* 2023;15:1145. DOI PubMed PMC

69. Cheng Y, Xiao X, Pan K, Pang H. Development and application of self-healing materials in smart batteries and supercapacitors. *Chem Eng J* 2020;380:122565. DOI
70. Ezeigwe ER, Dong L, Manjunatha R, Tan M, Yan W, Zhang J. A review of self-healing electrode and electrolyte materials and their mitigating degradation of lithium batteries. *Nano Energy* 2021;84:105907. DOI
71. Ma W, Wan S, Cui X, et al. Exploration and application of self-healing strategies in lithium batteries. *Adv Funct Mater* 2023;33:2212821. DOI
72. Lin WC, Yang YC, Tuan HY. Electrochemical self-healing nanocrystal electrodes for ultrastable potassium-ion storage. *Small* 2023;19:e2300046. DOI PubMed
73. Manju M, Thomas S, Lee SU, Kulangara Madam A. Mechanically robust, self-healing graphene like defective SiC: a prospective anode of Li-ion batteries. *Appl Surf Sci* 2021;541:148417. DOI
74. Pham PN, Wernert R, Aquilanti G, Johansson P, Monconduit L, Stievano L. Prussian blue analogues for potassium-ion batteries: application of complementary *operando* X-ray techniques. *Meet Abstr* 2022;MA2022-01:60. DOI
75. Fan Y, Tao T, Gao Y, et al. A self-healing amalgam interface in metal batteries. *Adv Mater* 2020;32:e2004798. DOI
76. Luo Y, Mou P, Yuan W, et al. Anti-liquid metal permeation separator for stretchable potassium metal batteries. *Chem Eng J* 2023;452:139157. DOI
77. Xue L, Gao H, Zhou W, et al. Liquid K-Na alloy anode enables dendrite-free potassium batteries. *Adv Mater* 2016;28:9608-12. DOI
78. Wang J, Hu M, Zhu Y, et al. Suppression of dendrites by a self-healing elastic interface in a sodium metal battery. *ACS Appl Mater Interfaces* 2023;15:16598-606. DOI
79. Zhang Y, Li Y, Shen W, Li K, Lin Y. Important role of atom diffusion in dendrite growth and the thermal self-healing mechanism. *ACS Appl Energy Mater* 2023;6:1933-45. DOI
80. Zhang B, Ren L, Wang Y, Xu X, Du Y, Dou S. Gallium-based liquid metals for lithium-ion batteries. *Interdiscip Mater* 2022;1:354-72. DOI
81. Lagrange P, El Makrini M, Guerard D, Herold A. Intercalation of the amalgams KHg and RbHg into graphite: reaction mechanisms and thermal stability. *Synth Met* 1980;2:191-6. DOI
82. Maji R, Salvador M, Ruini A, Magri R, Degoli E. A first-principles study of self-healing binders for next-generation Si-based lithium-ion batteries. *Mater Today Chem* 2023;29:101474. DOI
83. Guo P, Su A, Wei Y, et al. Healable, highly conductive, flexible, and nonflammable supramolecular ionogel electrolytes for lithium-ion batteries. *ACS Appl Mater Interfaces* 2019;11:19413-20. DOI
84. Jo YH, Li S, Zuo C, et al. Self-healing solid polymer electrolyte facilitated by a dynamic cross-linked polymer matrix for lithium-ion batteries. *Macromolecules* 2020;53:1024-32. DOI
85. Gan H, Zhang Y, Li S, Yu L, Wang J, Xue Z. Self-healing single-ion conducting polymer electrolyte formed via supramolecular networks for lithium metal batteries. *ACS Appl Energy Mater* 2021;4:482-91. DOI
86. Xie J, Ma L, Li J, et al. Self-healing of prussian blue analogues with electrochemically driven morphological rejuvenation. *Adv Mater* 2022;34:e2205625. DOI
87. Li Y, Zhang L, Zhang J, et al. Self-healing properties of alkali metals under “high-energy conditions” in batteries. *Adv Energy Mater* 2021;11:2100470. DOI
88. Domorenok E, Graziano P. Understanding the European green deal: a narrative policy framework approach. *Eur Policy Anal* 2023;9:9-29. DOI
89. Batteries: deal on new EU rules for design, production and waste treatment. European Parliament News. Available from: https://www.europarl.europa.eu/news/en/press-room/20221205IPR60614/batteries-deal-on-new-eu-rules-for-design-production-and-waste-treatment [Last accessed on 1 Aug 2023].
90. Johanna M. Council and parliament strike provisional deal to create a sustainable life cycle for batteries. 2022. Available from: https://www.consilium.europa.eu/en/press/press-releases/2022/12/09/council-and-parliament-strike-provisional-deal-to-create-a-sustainable-life-cycle-for-batteries/ [Last accessed on 1 Aug 2023].
91. Waldersee V, Amann C. BMW bets on design and recycling, not mining, to lower battery costs. Thomson Reuters. Available from: https://www.financedigest.com/bmw-bets-on-design-and-recycling-not-mining-to-lower-battery-costs.html [Last accessed on 1 Aug 2023].
92. Curtis T, Smith L, Buchanan H, Heath G. A circular economy for lithium-ion batteries used in mobile and stationary energy storage: drivers, barriers, enablers, and U.S. policy considerations. 2021. Available from: https://www.nrel.gov/docs/fy21osti/77035.pdf [Last accessed on 1 Aug 2023].
93. Liang H, Hou B, Li W, et al. Staging Na/K-ion de-/intercalation of graphite retrieved from spent Li-ion batteries: *in operando* X-ray diffraction studies and an advanced anode material for Na/K-ion batteries. *Energy Environ Sci* 2019;12:3575-84. DOI
94. Duc Pham H, Padwal C, Fernando JFS, et al. Back-integration of recovered graphite from waste-batteries as ultra-high capacity and stable anode for potassium-ion battery. *Batter Supercaps* 2022;5:e202100335. DOI
95. Zhu YH, Yin YB, Yang X, et al. Transformation of rusty stainless-steel meshes into stable, low-cost, and binder-free cathodes for high-performance potassium-ion batteries. *Angew Chem Int Ed* 2017;56:7881-5. DOI
96. Ye L, Wang C, Cao L, et al. Effective regeneration of high-performance anode material recycled from the whole electrodes in spent lithium-ion batteries via a simplified approach. *Green Energy Environ* 2021;6:725-33. DOI
97. Yuan X, Zhu B, Feng J, Wang C, Cai X, Qin R. Recent advance of biomass-derived carbon as anode for sustainable potassium ion

battery. *Chem Eng J* 2021;405:126897. DOI

98. Verma R, Singhbabu YN, Didwal PN, Nguyen A, Kim J, Park C. Biowaste orange peel-derived mesoporous carbon as a cost-effective anode material with ultra-stable cyclability for potassium-ion batteries. *Batter Supercaps* 2020;3:1099-111. DOI
99. Chen C, Wang Z, Zhang B, et al. Nitrogen-rich hard carbon as a highly durable anode for high-power potassium-ion batteries. *Energy Stor Mater* 2017;8:161-8. DOI
100. Xiao J, Min X, Lin Y, et al. A high-tortuosity holey graphene in-situ derived from cytomembrane/cytoderm boosts ultrastable potassium storage. *J Mater Sci Technol* 2023;139:69-78. DOI
101. Zhu Z, Zhong W, Zhang Y, et al. Elucidating electrochemical intercalation mechanisms of biomass-derived hard carbon in sodium-/potassium-ion batteries. *Carbon Energy* 2021;3:541-53. DOI
102. Shariati J, Haghtalab A, Mosayebi A. Fischer-Tropsch synthesis using Co and Co-Ru bifunctional nanocatalyst supported on carbon nanotube prepared via chemical reduction method. *J Energy Chem* 2019;28:9-22. DOI
103. Lotfabad EM, Ding J, Cui K, et al. High-density sodium and lithium ion battery anodes from banana peels. *ACS Nano* 2014;8:7115-29. DOI
104. Ren X, Xu S, Liu S, Chen L, Zhang D, Qiu L. Lath-shaped biomass derived hard carbon as anode materials with super rate capability for sodium-ion batteries. *J Electroanal Chem* 2019;841:63-72. DOI
105. Hao R, Lan H, Kuang C, Wang H, Guo L. Superior potassium storage in chitin-derived natural nitrogen-doped carbon nanofibers. *Carbon* 2018;128:224-30. DOI
106. Li H, Cheng Z, Zhang Q, et al. Bacterial-derived, compressible, and hierarchical porous carbon for high-performance potassium-ion batteries. *Nano Lett* 2018;18:7407-13. DOI
107. Cao W, Zhang E, Wang J, et al. Potato derived biomass porous carbon as anode for potassium ion batteries. *Electrochim Acta* 2019;293:364-70. DOI
108. Wu Z, Wang L, Huang J, et al. Loofah-derived carbon as an anode material for potassium ion and lithium ion batteries. *Electrochim Acta* 2019;306:446-53. DOI
109. Sun Y, Xiao H, Li H, et al. Nitrogen/oxygen co-doped hierarchically porous carbon for high-performance potassium storage. *Chemistry* 2019;25:7359-65. DOI
110. Liu M, Jing D, Shi Y, Zhuang Q. Superior potassium storage in natural O/N-doped hard carbon derived from maple leaves. *J Mater Sci Mater Electron* 2019;30:8911-9. DOI
111. Xu B, Qi S, Li F, et al. Cotton-derived oxygen/sulfur co-doped hard carbon as advanced anode material for potassium-ion batteries. *Chin Chem Lett* 2020;31:217-22. DOI
112. Zhang Z, Jia B, Liu L, et al. Hollow multihole carbon bowls: a stress-release structure design for high-stability and high-volumetric-capacity potassium-ion batteries. *ACS Nano* 2019;13:11363-71. DOI
113. Prabakar SJR, Han SC, Park C, et al. Spontaneous formation of interwoven porous channels in hard-wood-based hard-carbon for high-performance anodes in potassium-ion batteries. *J Electrochem Soc* 2017;164:A2012-6. DOI
114. He X, Sun H, Chen X, Zhao B, Zhang X, Komarneni S. Charging mechanism analysis of macerals during triboelectrostatic enrichment process: Insights from relative dielectric constant, specific resistivity and X-ray diffraction. *Fuel* 2018;225:533-41. DOI
115. Shan J, Wang J, Kiekens P, Zhao Y, Huang J. Effect of co-activation of petroleum coke and Artemisia Hedinii on potassium loss during activation and its promising application in anode material of potassium-ion batteries. *Solid State Sci* 2019;92:96-105. DOI
116. Gao C, Wang Q, Luo S, et al. High performance potassium-ion battery anode based on biomorphic N-doped carbon derived from walnut septum. *J Power Sources* 2019;415:165-71. DOI
117. Wang Q, Gao C, Zhang W, et al. Biomorphic carbon derived from corn husk as a promising anode materials for potassium ion battery. *Electrochim Acta* 2019;324:134902. DOI
118. Wang X, Zhao J, Yao D, et al. Bio-derived hierarchically porous heteroatoms doped-carbon as anode for high performance potassium-ion batteries. *J Electroanal Chem* 2020;871:114272. DOI
119. Nagmani, Verma P, Puravankara S. Jute-fiber precursor-derived low-cost sustainable hard carbon with varying micro/mesoporosity and distinct storage mechanisms for sodium-ion and potassium-ion batteries. *Langmuir* 2022;38:15703-13. DOI PubMed
120. Yuan X, Zhu B, Feng J, Wang C, Cai X, Qin R. Biomass bone-derived, N/P-doped hierarchical hard carbon for high-energy potassium-ion batteries. *Mater Res Bull* 2021;139:111282. DOI
121. Hu Z, Liu Z, Zhao J, Yu X, Lu B. Rose-petals-derived hemispherical micropapillae carbon with cuticular folds for super potassium storage. *Electrochim Acta* 2021;368:137629. DOI
122. Xu Z, Du S, Yi Z, et al. Water chestnut-derived slope-dominated carbon as a high-performance anode for high-safety potassium-ion batteries. *ACS Appl Energy Mater* 2020;3:11410-7. DOI
123. Tao L, Liu L, Chang R, He H, Zhao P, Liu J. Structural and interface design of hierarchical porous carbon derived from soybeans as anode materials for potassium-ion batteries. *J Power Sources* 2020;463:228172. DOI
124. Luo H, Chen M, Cao J, et al. Cocoon silk-derived, hierarchically porous carbon as anode for highly robust potassium-ion hybrid capacitors. *Nanomicro Lett* 2020;12:113. DOI PubMed PMC
125. Yang M, Dai J, He M, Duan T, Yao W. Biomass-derived carbon from Ganoderma lucidum spore as a promising anode material for rapid potassium-ion storage. *J Colloid Interface Sci* 2020;567:256-63. DOI PubMed
126. Tian S, Guan D, Lu J, et al. Synthesis of the electrochemically stable sulfur-doped bamboo charcoal as the anode material of potassium-ion batteries. *J Power Sources* 2020;448:227572. DOI

127. Chen J, Chen G, Zhao S, et al. Robust biomass-derived carbon frameworks as high-performance anodes in potassium-ion batteries. *Small* 2023;19:e2206588. DOI
128. Xu L, Guo W, Zeng L, et al. V_3Se_4 embedded within N/P co-doped carbon fibers for sodium/potassium ion batteries. *Chem Eng J* 2021;419:129607. DOI
129. Xue Q, Li D, Huang Y, et al. Vitamin K as a high-performance organic anode material for rechargeable potassium ion batteries. *J Mater Chem A* 2018;6:12559-64. DOI
130. Wu Z, Zou J, Zhang Y, et al. Lignin-derived hard carbon anode for potassium-ion batteries: interplay among lignin molecular weight, material structures, and storage mechanisms. *Chem Eng J* 2022;427:131547. DOI
131. Cheng G, Zhang W, Wang W, et al. Sulfur and nitrogen codoped cyanoethyl cellulose-derived carbon with superior gravimetric and volumetric capacity for potassium ion storage. *Carbon Energy* 2022;4:986-1001. DOI
132. Li W, Li Z, Zhang C, et al. Hard carbon derived from rice husk as anode material for high performance potassium-ion batteries. *Solid State Ionics* 2020;351:115319. DOI
133. Ronsse F, Nachenius RW, Prins W. Chapter 11 - carbonization of biomass. In: Recent advances in thermo-chemical conversion of biomass. Amsterdam, The Netherlands: Elsevier; 2015. pp. 293-324. DOI
134. Abramova EN, Marat N, Rupasov DP, Morozova PA, Kirsanova MA, Abakumov AM. Hard carbon as a negative electrode material for potassium-ion batteries prepared with high yield through a polytetrafluoroethylene-based precursor. *Carbon Trends* 2021;5:100089. DOI
135. Li Y, Adams RA, Arora A, et al. Sustainable potassium-ion battery anodes derived from waste-tire rubber. *J Electrochem Soc* 2017;164:A1234-8. DOI
136. Trano S, Corsini F, Pascuzzi G, et al. Lignin as polymer electrolyte precursor for stable and sustainable potassium batteries. *ChemSusChem* 2022;15:e202200294. DOI PubMed PMC
137. Manarin E, Corsini F, Trano S, et al. Cardanol-derived epoxy resins as biobased gel polymer electrolytes for potassium-ion conduction. *ACS Appl Polym Mater* 2022;4:3855-65. DOI PubMed PMC